

Fall 12-2016

## Laboratory Development of a Self-Powered Fontan for Treatment of Congenital Heart Disease

Arka Das  
*Embry-Riddle Aeronautical University*

Follow this and additional works at: <https://commons.erau.edu/edt>



Part of the [Biomedical Devices and Instrumentation Commons](#)

---

### Scholarly Commons Citation

Das, Arka, "Laboratory Development of a Self-Powered Fontan for Treatment of Congenital Heart Disease" (2016). *Doctoral Dissertations and Master's Theses*. 296.  
<https://commons.erau.edu/edt/296>

This Thesis - Open Access is brought to you for free and open access by Scholarly Commons. It has been accepted for inclusion in Doctoral Dissertations and Master's Theses by an authorized administrator of Scholarly Commons. For more information, please contact [commons@erau.edu](mailto:commons@erau.edu).

LABORATORY DEVELOPMENT OF A SELF-POWERED FONTAN FOR  
TREATMENT OF CONGENITAL HEART DISEASE

by

Arka Das

A Thesis Submitted to the College of Engineering Department of Mechanical  
Engineering in Partial Fulfillment of the Requirements for the Degree of  
Master of Science in Mechanical Engineering

Embry-Riddle Aeronautical University  
Daytona Beach, Florida  
November 2016

LABORATORY DEVELOPMENT OF A SELF-POWERED FONTAN FOR  
TREATMENT OF CONGENITAL HEART DISEASE

by

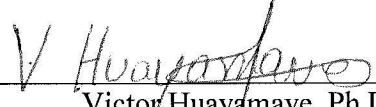
Arka Das

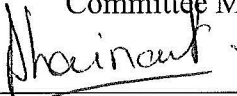
This thesis was prepared under the direction of the candidate's Thesis Committee Chair, Dr. Eduardo A. Divo, Daytona Beach Campus, and Thesis Committee Members Dr. Jean M. Dhainaut, Daytona Beach Campus, and Dr. Victor Huayamave, Daytona Beach Campus, and has been approved by the Thesis Committee. It was submitted to the Department of Mechanical Engineering in partial fulfillment of the requirements for the degree of Master of Science in Mechanical Engineering

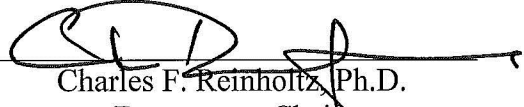
Thesis Review Committee:


  
Eduardo Divo, Ph.D.  
Committee Chair

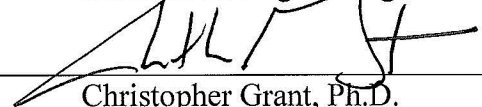
  
Jean-Michel Dhainaut, Ph.D.  
Committee Member

  
Victor Huayamave, Ph.D.  
Committee Member

  
Jean-Michel Dhainaut, Ph.D.  
Graduate Program Chair,  
Mechanical Engineering

  
Charles F. Reinholtz, Ph.D.  
Department Chair,  
Mechanical Engineering

  
Maj Mirmirani, Ph.D.  
Dean, College of Engineering

  
Christopher Grant, Ph.D.  
Associate Vice President of Academics

11/28/16  
Date

## **Acknowledgements**

I cannot express enough gratitude to my thesis advisor Dr. Eduardo Divo for all of his complete support and advice which he provided throughout my research work. He not only guided me in completing my research work but also he showed me the path to shape my life in a better manner by helping me to choose the correct decisions at crucial times. I will be forever grateful to him. I would also like to thank my committee members Professor Jean M. Dhainaut, Professor Victor Huayamave and Dr. William Decampoli for their insight and feedback during my research. My heartfelt thanks go to Kristin Sverrisdottir for her complete support throughout all these years. Without your friendship this journey of mine in abroad would not have been this awesome and pleasant. You always stood beside me. The time we spent together is invaluable to me. A special thanks to Rebecca Gold for editing my writing on such short notices. I really appreciate your hard work. I am also thankful to the whole senior design group of 2015-16 and Anthony Khoury and Jake Tibbets for their diligent work to make this research successful. I wish you all the best of luck through your endeavors. I am so grateful to my family, especially my parents and my late grandmother “Priti Kana das” for my upbringing and for being there for me during all my hard times. Last but not the least I would like to thanks all my friends especially Bhushan, Sultan and Alex to make my graduate school life awesome.

## Abstract

Researcher: Arka Das  
Title: Laboratory Development of a Self-Powered FONTAN for Treatment of Congenital Heart Disease

Institution: Embry-Riddle Aeronautical University  
Degree: Master of Science in Mechanical Engineering  
Year: 2016

Around 8% of all newborns with a Congenital Heart Defect (CHD) have only a single functioning ventricle. The Fontan operation has served as a palliation for this anomaly for decades, but the surgery entails multiple complications and survival rate is less than 50% by adulthood. A rapidly testable novel alternative is proposed by creating a bifurcating graft, or Injection Jet Shunt (IJS), used to “entrain” the pulmonary flow and thus provide assistance while reducing the caval pressure. A benchtop Mock Flow Loop (MFL) is configured to validate this hypothesis. The MFL is based on a Lumped-Parameter Model (LPM) of the Fontan circulation and is comprised of upper and lower systemic as well as left and right pulmonary compartments. Needle valves are used to accurately replicate vascular resistance (R) while compliance chambers are used to mimic vascular compliance values (C). The Fontan MFL is driven with cardiac pulsatility provided by a Harvard Apparatus medical pump. Patient-specific models of the centerpiece of the MFL along with the grafts (IJS) are produced via 3D printing. Baseline values are validated against patient-specific waveforms. Flow and pressure sensor data at specific points in the MFL are acquired via a National Instruments multichannel data acquisition board and processed using LabView. Several IJS nozzle diameters are tested to validate the hypothesis and optimize the improvement.

## Table of Contents

	Page
Thesis Review Committee .....	ii
Acknowledgements.....	iii
Abstract .....	iv
List of Tables .....	viii
List of Figures .....	ix
Chapter	
I    Introduction.....	1
Circulatory Pattern .....	1
Cardiac Cycle.....	2
Hypo Plastic Left Heart Physiology .....	4
Palliative Procedure .....	5
Roles of Valves and Pulsatile Right Atria .....	7
Post Fontan Paradox and Fenestration .....	9
II    Review of the Relevant Literature .....	11
Physiological Parameters to construct the Loop.....	13
Blood Volumes .....	13
Frank Starling Law .....	13
Vascular Compliance.....	14
Vascular Resistance.....	16
Hypothesis.....	17

III	Methodology .....	19
	Pump .....	21
	Vascular Compliance .....	23
	Vascular Resistance .....	26
	Injection Jet Shunt.....	27
IV	Experimentation .....	29
	Components .....	29
	Test Rig/Table Top .....	29
	Harvard Apparatus Pump .....	29
	Compliance Chamber.....	30
	Resistors .....	30
	Flow Meters .....	31
	Pressure Sensors.....	32
	Data Acquisition System.....	33
	cDAQ chassis.....	33
	Digital module .....	34
	Analog module.....	35
	Software .....	35
	Calibration of Sensors.....	35
	Process .....	36
IV	Results.....	39
	Baseline case .....	41
	IJS with Open cannula .....	42

	IJS with partially closed cannula .....	43
V	Discussion, Conclusions, and Recommendations.....	44
	Discussion.....	44
	Conclusions.....	45
	Future work.....	45
	References.....	47
Appendices		
A	Bibliography .....	#
B	Permission to Conduct Research .....	53
C	Data Collection Device.....	55
D	Calibration Curves .....	56
E	Raw Data.....	60



## List of Tables

	Page
Table	
3.1 Anatomically Derived Non-Dimensional Parameter .....	22
3.2 Anatomically Derived Frequency and Individual Volumetric Flow rate .....	23
3.3 Compliances for body surface Area = $0.67\text{m}^2$ .....	24
3.4 Utilized Vascular compliance .....	24
3.5 Effective radius for desired compliance .....	25
3.6 Pressure drop .....	26
5.1 Results .....	39

## List of Figures

	Page
Figure	
1.1 Cardiac cycle event.....	3
1.2 Cardiovascular anatomy for Normal Human Heart and Ailing Heart under HLHS .....	5
1.3 HLHS and Fontan Circulation .....	6
2.1 Frank Starling Law. ....	14
3.1 Lumped Parameter Model without IJS. ....	20
3.2 Lumped Parameter Model with IJS .....	20
3.3 Harvard Apparatus Pump.....	21
3.4 2D CAD model of IJS.....	27
3.5 Placement of IJS in MFL. ....	28
3.6 IJS Prototypes. ....	28
4.1 Compliance chamber in MFL. ....	30
4.2 Resistor in MFL. ....	31
4.3 Flow meter installed in MFL .....	32
4.4 Pressure Sensor installed in MFL .....	33
4.5 Labelled diagram of MFL showcasing components of lumped parameter.....	37
4.3 Labelled diagram of MFL Flow showing position of sensors .....	38
4.3 Labelled diagram of MFL Flow showing compliance chamber .....	38
5.1 Figure showing pressure at IVC for baseline and Qp/Qs ratio and pressure at IVC for various IJS with fully open Inlet cannula.....	43

5.2	Figure showing Pressure at IVC for baseline and $Q_p/Q_s$ ratio and Pressure at IVC for various IJS with partially closed Inlet cannula.....	44
5.3	Baseline case with Flow rates .....	44
5.4	Baseline case with Pressure plots .....	45
5.5	Flow rate plot for 2mm IJS with fully open Inlet cannula.....	45
5.6	Pressure plot for 2mm IJS with fully open Inlet cannula.....	46
5.7	Flow rate plot for 2mm IJS with partially open Inlet cannula .....	46
5.8	Pressure plot for 2mm IJS with partially open Inlet cannula.....	47

## **Chapter I**

### **Introduction**

#### **Circulatory pattern**

The heart is located roughly in the center of the chest cavity and protected by a membrane called the pericardium. Venous blood from the body enters the right atrium. It flows to the right ventricle through the tricuspid valve. The right ventricle contracts and the tricuspid valve closes which forces to open the pulmonary valve. Then deoxygenated blood flows through pulmonary artery. This branches immediately, carrying blood to the right and left lungs. Carbon dioxide is released from hemoglobin, diffuses out of blood cells and capillaries around the alveoli and into the interior of the alveoli, as oxygen diffuses from the alveoli, into the capillaries and blood cells and binds to hemoglobin. The overall process is called respiration. The capillary beds of the lungs are drained by venules that are the tributaries of the pulmonary veins. Two pulmonary veins draining from each lung carry oxygenated blood to the left atrium of the heart. Now the oxygenated blood flows to the left ventricle through mitral valve. Contraction of the left ventricle closes the mitral valve and opens the aortic valve at the entrance to the aorta and other two openings lead to the right and left coronary arteries, which supply blood to the heart itself. Coronary arteries arise within the heart and pass directly out to its surface and extends down across it. These arteries supply blood to the network of capillaries that penetrate every portion of the heart. These capillaries drain into two coronary veins which returns back to right atrium. The remainder of the blood flow coming out of aorta goes to the systemic circulation. The systemic circulation is a branching system of arteries that lead to all parts of the body. These arteries lead to capillaries and those in

turn drain blood to venules. Veins draining blood of upper portion of the body lead to the superior vena cava while veins draining blood of lower portion of the body lead to the inferior vena cava. Both superior and inferior vena cava lead to the right atrium.

### **Cardiac Cycle**

The cardiac cycle refers to the sequence of events from the beginning of one heart beat to the initiation of the next beat. There are two major phases of a cardiac cycle i.e. diastole and systole. The heart rate determines the frequency of the cardiac cycle by expressing as "*heart beats per minute*". Totally there are five major stages in a cycle.

In the first stage, the atrium contracts and the pressure rises across the atrioventricular (AV) valve. The AV valve opens up which makes the blood fill the right ventricle. After the atrial contraction the pressure falls down and the valve closes gradually. By the end of this stage the right ventricle reaches its maximum volume, known as "End Diastolic Volume (EDV)".

In the second stage, the right ventricle contracts which increases the ventricular pressure to a great extent and the volume remains constant. This stage is also known as "Isovolumetric Contraction".

The third stage is known as "Rapid ejection," which occurs when the pressure inside the ventricle exceeds the pressure in the pulmonary arteries (10 mmHg) and Aorta (80 mmHg) causing the blood to eject out of the ventricles. The rate of ejection is higher during the beginning of the stage but gradually slows down as the systole progresses. In this stage, ventricular pressure stays a little higher than the pulmonary artery and aortic

pressure. Also, a gradual decrease in atrial pressure with the rapid decrease in the ventricular volume is also observed.

In the fourth stage, the ventricular pressure falls below the pulmonary and aortic pressure causing a reduced ventricular ejection rate. This flow continues for a short span of time due to inertia.

In the fifth stage, all the AV valves and semilunar valves close. The ventricles gets relaxed and the ventricular pressure drops below 120 mmHg. During this stage the blood gets pumped to the body through the systemic circulation.

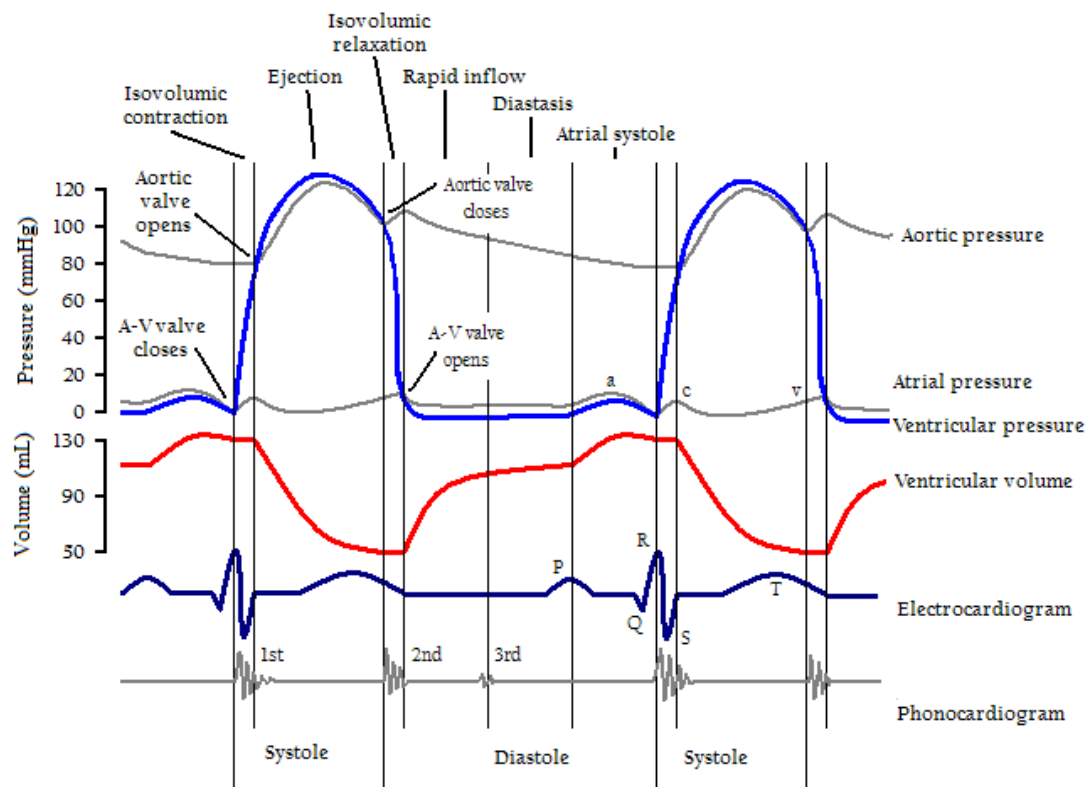


**Figure 1.1:** This figure describes the cardiac cycle events

### **Hypo Plastic Left Heart Physiology**

Hypo-plastic left heart syndrome (HLHS) is a very rare and complex congenital heart anomaly where the malformation of the left ventricle and aorta render those minimally or non-functional. In this altered physiology, the aortic and mitral valves are under developed to cause sufficient amount of blood flow. The blood from the left atrium flows to the right ventricle through a defective interatrial septum. This defective interatrial septum is also a congenital defect, which is known as “Atrial Septal defect”. Therefore the right ventricle is overloaded as it pumps both oxygenated and deoxygenated blood to parallel pulmonary and systemic circulations.

Also the ductus arteriosus usually closes within eleven days after birth hence blood flow will be eventually blocked after that period. This may lead to death of the baby due to severe lack of oxygenated blood flow in the systemic circulation. HLHS can be very fatal, though it may be prevented through surgical interventions. Before the surgery takes place, less oxygenated air is passed through the infants suffering from HLHS which helps the ductus to remain open and make the blood flow to the systemic circulation.

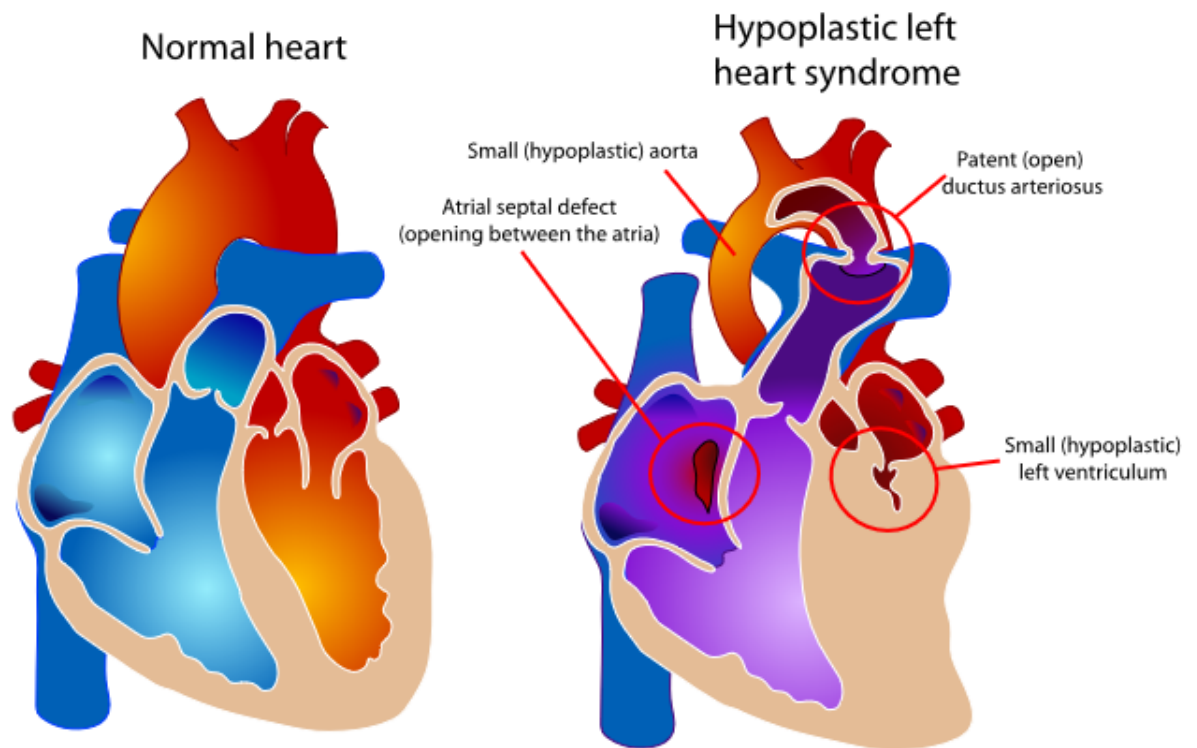


**Figure 1.2: This figure shows the difference in Human cardiovascular anatomy for a normal Human Heart and ailing Heart suffering from HLHS**

### **Palliative Procedure**

A surgery is performed in the following three sequential stages to mitigate the flow pattern of HLHS:

#### *Stage 1: Norwood*

In this stage, atrial septectomy is performed and the hypoplastic aorta is reconstructed and connected to the right ventricle in place of the pulmonary root. A Blalock Taussig (BT) shunt is implanted between the innominate artery and the pulmonary arteries to create a parallel path between the systemic circulation and the pulmonary circulation. The Norwood procedure is performed very shortly after birth.



Stage 2: Glenn

In this stage, the superior vena cava (SVC) is disconnected from the right atrium and connected directly to the right pulmonary artery and the BT shunt is disconnected. The main purpose of this surgery is to send the deoxygenated blood flow from the upper systemic circulation to the pulmonary circulation. The Glenn procedure is performed between three and six months after the first stage.

Stage 3: Fontan

In this stage, the inferior vena cava (IVC) is disconnected from the right atrium and connected directly to the pulmonary arteries for a Total Cavopulmonary Connection (TCPC), [1]. This results in total passive drainage of the caval blood flow to the pulmonary circulation and therefore relieving the single ventricle from pumping blood to the pulmonary circulation, see Fig. 2. The atrial septal defect is closed. The Fontan procedure is performed around six months to a year after the second stage.

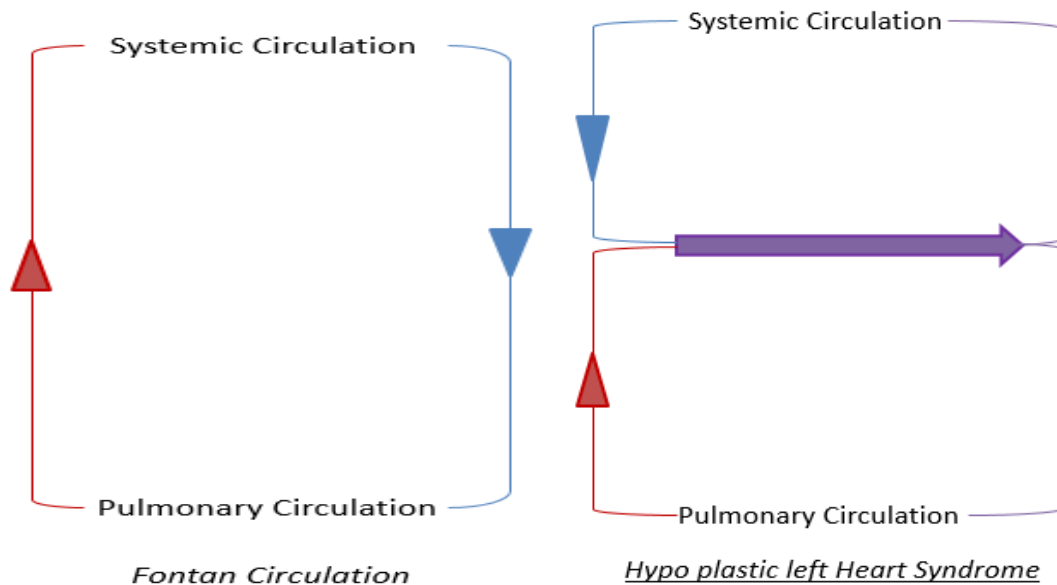


**Figure 1.3: Comparison between Hypoplastic Left Heart Syndrome and Fontan Circulation**

### **Role of Valves and Pulsatile Right Atria**

During the course of time the implementation of valves were investigated repeatedly. It was found that stenotic valves were the main reasons for conduit failure. Flexibility and plasticity of the valves were also a crucial point of investigation. Many research works also revealed that atriopulmonary conduits were not affected by the implementation of valves rather affected by the Right Atrium (RA) pressure.

Now the next point of concern was the inclusion of RA in an univentricular circulation because the RA was pulsatile and developing high pressures which often lead to cardiac malfunctions like “arrhythmias”, right pulmonary vein obstructions. The original atriopulmonary (AP) connection also made the patient response to the altered hemodynamics very unpredictable. This procedure also lead to anomalies like atrial flutter and fibrillations.

Three different procedures of practicing the Fontan surgery are currently available. Each is associated with certain amount of complications which are discussed below

### **Intra Atrial Total Cavopulmonary Connection (lateral tunnel)**

In 1988, de laval conducted an *in-vitro* experiments which showed that atrial chamber of the conventional atriopulmonary procedure induces turbulence in the flow which in turn increases the resistance to the circulation. From those experiments he developed an alternative approach to the existing classical AP procedure. In this, the most of the RA is excluded hence this procedure is called as Intra-atrial Total Cavopulmonary Connection (TCPC). This TCPC is mainly constructed by end to side anastomosis of the

Superior Vena Cava (SVC) and Right pulmonary Artery (RPA). This intra-atrial conduit was made with composite material and a synthetic graft to strait the Inferior Vena Cava (IVC) to the inferior side of RPA through a part of RA wall.

### **Extra cardiac Total Cavopulmonary Connection**

Around 1990, Marcelleti and colleagues developed a new alternative procedure to the existing lateral tunnel method. In this procedure an extra cardiac conduit was used to connect IVC to PA through outside of the heart. Hence this procedure is called as “Extra cardiac Total Cavopulmonary Connection”. The shunt was made of complex composite material and long homograft was used.

### **Attributes of Three different Fontan Procedures**

In lateral tunnel shows a decreased risk of atrial thrombosis and arrhythmias. Also, this conduit procedure showcased less energy losses and turbulence effect. This procedure has aortic cross clamping and excessive intra- atrial suture lines. The intra-atrial baffle has the tendency to generate thrombogenicity.

The extra cardiac total cavopulmonary process has showcased many advantages. This procedure can be performed on patients without arresting their heart and without cardiopulmonary bypass. Also, there is no need for extensive atrial suture lines and aortic cross-clamping. In this process, the RA is totally avoided and as a result it does not get exposed to high venous pressure and high wall stress. This leads to less probability of arrhythmias, embolization, atrial flutter and fibrillation.

The disadvantage of this procedure is the inability for growth of graft. Also implanted homografts are extremely expensive.

### **Research modalities**

The discovery of TCPC highlighted the importance of investigation of parameters like streamline pattern, reduced turbulence, and absence of stagnation in the blood flow. Many techniques were reinvestigated to improve the flow pattern and reduce energy losses. As it is a single ventricular flow, the energy maintenance was a very crucial factor. Other important areas to concern from the surgical point of view were bifurcation angles, the degree of offset between anastomoses, material properties and geometry of the shunt.

### **Post Fontan Paradox and Fenestration**

A "fenestration" is a hole that is usually punctured on the right atrium to relief the high pressure developed in the Fontan circuit. Due to this, the pulmonary vascular resistance increases and the ventricular function decreases, altering the hemodynamics, [2]. In addition, fenestration can also lead to severe congestion of the SVC and/or the IVC, arrhythmias, ventricular dysfunction, unusual clinical syndromes of protein-losing enteropathy (PLE), and plastic bronchitis. The Fontan procedure often lead to multiple complications like chronic illness, severe reduction in quality of life, and chances of survival of less than 50% by adulthood [3-10]. In the Fontan circulation, the blood flows passively from the systemic circulation return to the pulmonary circulation in the absence of the second pumping chamber. This circulatory pattern can fail, even in patients with relatively good ventricular function. Pharmacological and other therapies have variable

success [11-14]. The probability of successful outcome with heart transplantation is low [15-19]. Some have suggested “assisting” the Fontan circulation using an implanted, intravascular, synthetic, externally powered pump [20-23]. Such pumps are under laboratory investigation, but problems associated with these pumps (stroke, infection, pump failure) still remain. The solutions to these problems are still many years away.

## Chapter II

### Review of the Relevant Literature

Mock flow loop (MFL) is a bench top model which replicates the human circulatory system mechanically for carrying out various *in vitro* experiments. Generally these MFL consist of a pump, a preloaded tank, resistance valves and accumulators. These resistance valves and accumulators account for the vascular resistance and vascular compliance provided by the circulation. The tank replicates the ventricular bed for the pump. The pump can be either pulsatile or continuous depending on the working parameters. A detailed literature survey is conducted to determine these important parameters and is presented in this section.

Very first generation MFLs were primarily used for *in vitro* analysis of artificial heart valves where the heart is mimicked by a stepper motor [25]. Also, many setups used transparent and flexible ventricles for vulvar flow analysis [26-30]. These MFLs were very rudimentary, comprised of very limited elements.

An MFL as discussed in [31] is comprised of both systemic and pulmonary circulations. Compressed air was used as the working fluid for ventricles and huge water columns were used to maintain the pressure in the pulmonary arteries. Here, the pressure was controlled by the column of water present in the tube, but this tall water column induced an undesirable inertia effect in the loop. A flow meter was used to check the equality in the amount of flow rate in both systemic and pulmonary circulation.

In [32] an MFL consisting of only systemic circulation was developed. The whole system was submerged into the water filled Perspex box. This Perspex box was

connected to the Windkessel model, which can be tuned by the adjustable air volume. Each branch of the circulation had a separate resistor. The pulsatile pressure was applied by the cam to the whole system.

A concise summary of the design and analysis of MFL is presented in [33]. It describes the features like resistance, compliance, inductance, pulmonary circulations, cardiac connections, etc. and their working parameters.

There is a wide variety of MFLs available. These can vary from two element lumped parameter models to five element lumped parameter models. A study conducted in [34] compares the accuracy between results produced by a MFL with physiological values produced by natural human circulation. It was found that with the addition of each element in the loop the generated results were becoming more accurate and resembling the physiological values. However, the anomaly was observed upon addition of the fourth element into the loop. It did not improve the results by any scale with respect to the three element lumped parameter model. The results improved significantly with the inclusion of fifth element into the loop.

An MFL was designed for infants in [34-35]. In this in vitro experiment the physiological parameters followed were of infants. The generated results were compared with the values for an adult case. The results of this study sets up the baseline reference criteria for any infant or neonatal cardiovascular simulation.

In [36] an MFL containing only a systemic circulation is developed. This MFL consisted of a Frank Starling loop to analyze the hemodynamic and ventricular pressure volume (PV) behavior for different cardiac assist provided to the loop. The vascular resistance was made up of a compliant latex tube in a sealed chamber.

A full scale MFL was developed in [37] to simulate the normal and diseased heart conditions. The test rig had the ability to produce the Frank Starling effect but was not capable of measuring the ventricular volume. This loop had the ability to measure a wide extent of flow and pressure values accurately for the ailed and normal heart conditions.

Though many MFLs were previously constructed to exactly simulate the systemic circulation of the human physiology and to test various cardiovascular device, a very minimal amount of work has been carried out to replicate the HLHS and to test any modified palliative surgery procedures. Also, most of the loops lack a precisely controlled variable compliance chamber.

### **Physiological Parameters to construct the loop**

#### **Blood volumes**

The majority of the volume of blood is stored in the veins of the human body as veins are more compliant than arteries. A typical adult can approximately hold 5 liters of blood volume in his system. A study has been conducted in [38] to determine the effect of body postures on the blood circulation. It has been found that cardiac output in the supine position is around 7.8 L/min, while for the sitting position it is 5.9 L/min. It is also mentioned that cardiac output gets increased by 51%.

A neonatal MFL is created in [39] which had a total volume of 200mL, which resembled the blood volume of a neonate weighing 2.7 kg. This loop had simulated only main venous flow, central veins and the right atrium.

In [40] a detailed view of MFL including the parameters like vascular resistance, vascular compliance and ventricular volumes were provided.



### Frank Starling Law

Frank Starling Law states that human heart has the ability to increase its stroke volume with the increase in volume of blood filling the heart. By this law it can also be stated that heart works harder to pump more blood hence there is a resistance to backflow. This also explains that due to the increased volume of blood the ventricular wall stretches during the ventricular preload causing the ventricle to contract more.

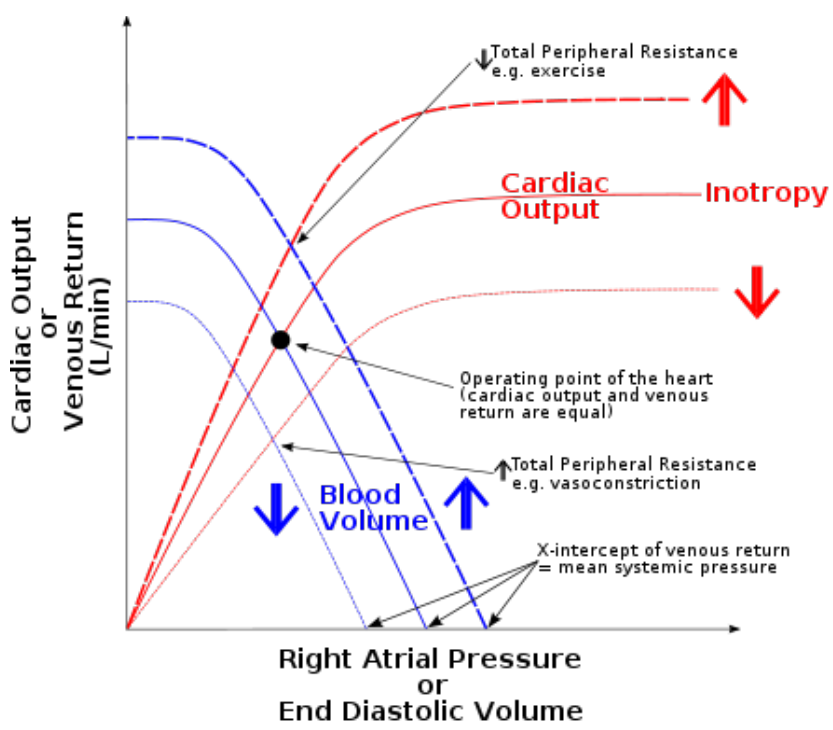


Figure 2.1: This figure shows the Frank Starling Law

### Compliance

By definition compliance means the change of volume of liquid in a chamber with respect to the change of pressure in the same chamber.

$$\text{Compliance} = \text{Change in volume (mL)} / \text{Change in Pressure (mmHg)}$$

Compliance is inversely proportional to Elastance. The veins are much more compliant than arteries, and as a result they can hold a huge amount of blood in them. The ventricular compliance determines the end diastolic pressure for a given end diastolic volume.

In [39] the compliance was achieved by trapping the air above the working fluid inside each chamber. All four chambers, i.e. systemic arterial, systemic venous, pulmonary arterial and pulmonary venous, were variable as the volume of trapped air could be changed.

The same MFL as discussed in [40] was developed for a hemolysis study of the Ventricular Assist Device (VADs). This loop utilized a compliance chamber which was made of sacs. The sac was submerged into the chamber. The chamber was just big enough to fit a sac inside it, hence the compliance was restricted by the size of the chamber.

A new design of compliance chamber was presented in this study [41]. This design is based on a spring mass system. A conical seat was made to fit the spring exactly in the center position of the piston. The spring constant was calculated by using the following equation:

$$K = \frac{A_c^2}{C} \quad (1)$$

Where K is the spring constant,  $A_c$  is the Area of the Piston rod and C is the desired compliance value. From the equation it can be seen that variable compliance could be achieved by using different diameter springs.

A study had been conducted to analyze the effect of arterial compliance during intra -aortic balloon counter pulsation. A variable air based compliance chamber was used in this MFL setup. The compliance value was calculated by

$$C = -\frac{dV}{dP} \quad (2)$$

The whole process was considered as isothermal, hence

$$C = \frac{V}{P} \quad (3)$$

A compliance chamber made of flexible rubber walls was designed in [42]. This design had a clear plastic which was used to attach to the distal end of the ventricle. The flexible rubber wall helped the flow to dampen the pulse pressure. The variable compliance was achieved by changing the flexible diaphragm to match the required compliance value.

In this MFL a compliance chamber was developed for simulating the complacency of lungs [43]. This chamber was made of a soft and compliant polyurethane bag which was trapped in an air tight rigid box. This box was supplied with compressed air to change the compliance value by varying the volume of the bag.

Previously, many compliance chambers were developed based on the principle that the air tight tanks were used to trap the air above the working fluid and the volume of the entrapped air used to determine the compliance value in [44]. However, for all of these designs the MFL have to be shut down each time to change the compliance. A modified technique had been found in [Litwak et al] where an air valve is placed at the top of the chamber to control the air intake hence the compliance of the circuit.

To determine the corrected compliance value

$$C = \frac{dV_{fluid}}{dP_{fluid}} = \frac{V_{air}}{P_{air}} = \frac{V_{tank} - A_{tank} \cdot h_{fluid}}{P_{fluid} - \rho \cdot g \cdot h_{fluid}} \quad (4)$$

Where  $C$  = Desired compliance,  $V_{\text{tank}}$  = Volume of the Tank,  $V_{\text{air}}$  = Volume of air. An extensive in depth study of estimation of arterial compliance had been carried out and compared with previously published results in [45]. In this procedure four two-element lumped parameter model along with time decay and the area, the two-area method was implemented. It also accounted for fluid friction and inertia. In this study three element LPM with low frequency impedance and integral method was considered. It was found that all the methods associated with two-element LPM generated error less than 10%. Finally, as a result, it was inferred that for the systemic arterial tree two-element LPM model worked much accurately with low frequencies whereas three-element LPM models worked much more accurately with higher frequencies.

### **Vascular Resistance**

The vascular resistance plays a very crucial role in the whole circulatory system. Different body parts exhibits the resistance in a different way. The aorta offers very little resistance to the blood flow whereas the systemic circulation provides a high amount of resistance to the blood flow due to the presence of small veins and arteries. Hence, the pressure drop across the aorta is lesser than the systemic circulation. Human body has the ability to change the effective resistance provided by the vasculature to direct the blood flow in different directions. The key parameters which govern the resistance are:

Hence

$$R \propto \frac{n \cdot L}{r^4} \quad (5)$$

Radius of the vasculature ( $r$ )

Length of the vasculature ( $L$ )

Viscosity of the fluid ( $\eta$ )

Very primarily the resistance was replicated by electronically controlled pinch valve in [3] and [46].

A new design of vascular resistance was found in [16]. This resistance was based on plate rotated about pivot to restrict the flow through the tube. The amount of restriction depends on the angle of rotation of a plate mounted on pivot. The plate is connected with a bellow. When the aortic or pulmonary pressure increased, the bellow was forced to contract which pulled the lever arm, and then the valve plate rotated about the pivot.

The resistance was calculated by

$$\Delta P = R \cdot Q \quad (6)$$

$$R = \frac{8 \cdot \mu \cdot L_R \cdot \pi}{A_R^2} \quad (7)$$

## Hypothesis

A novel, innovative, rapidly testable alternative is proposed to achieve the same endpoints as a synthetic pump in the Fontan circulation. Through this procedure the reserve mechanical energy of the heart itself is tapped to “assist” the Fontan circulation by creating a novel bifurcating graft, henceforth called the Injection Jet Shunt (IJS), see Fig 2. A new, technically straightforward surgical operation is proposed in which this graft, originating from either the ventricle or aorta, bifurcates with each tapered distal limb sutured into the pulmonary arteries (PA) in such a way that flow is directed parallel to each PA and the energy and momentum of this flow is efficiently transferred. The principle of this process is based on the “injection jet” mechanism in fluid mechanics that

has wide industrial applications in well pumps, enhanced oil recovery, and water eductors on underwater archeological sites [24], but this concept has never been used to address the failing Fontan paradox. The hypothesis is as follows: The inclusion of an IJS of suitable geometry into the “failing Fontan” circulation can (1) decrease IVC pressure and (2) increase systemic oxygen delivery while limiting the obligatory left-to-right shunt through the graft to a clinically acceptable value. The approach challenges the existing paradigm that a synthetic pump is required to assist the Fontan circulation. It addresses the critical barriers to progress in this field by offering an alternative, effective palliation for the failing Fontan while delaying or circumventing the need for heart transplantation and implantation of synthetic pumps with their well-known complications.

## **Chapter III**

### **Methodology**

The bench top Mock Flow Loop (MFL) was modeled to resemble the cardiovascular system of the target population, i.e. 6 months old babies with an ailing heart for the palliative procedure. This was accomplished using a Lumped-Parameter Model (LPM) of the Fontan circulation anatomy with four branches, or lumps, representing the upper and lower systemic circulations as well as the left and right pulmonary circulations, shown in Fig. 3. This is also referred as a “Base line model”. Each analogous lump accounts for both the arterial and venous vasculatures found within the physiological anatomy. In the figure, a four way junction mimicked the atrio-pulmonary conduit based Fontan procedure. Each section of the systemic circulation, i.e. upper and lower and pulmonary circulation, i.e. right and left, is represented by two elements, i.e. Resistance (R) and Compliance (C) lumped parameters. Here the heart is represented as a voltage source. In the next figure it is shown that how the IJS is getting connected with RPA and LPA and the heart. It is important to note that the MFL is not designed as an artificial equivalent of patient anatomy as the development of such a construct is infeasible due to the complexities of the cardiovascular system. Instead, the MFL represents an observable analogy to human anatomy, producing flow behavior that is physiologically relevant and accurate.

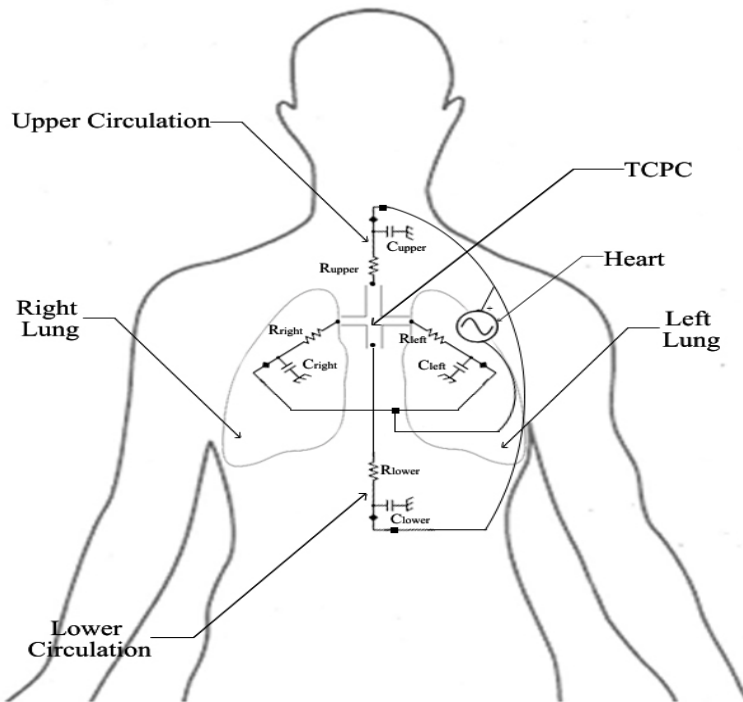


**Figure 3.1: Lumped Parameter model of Atriopulmonary based Fontan Procedure**

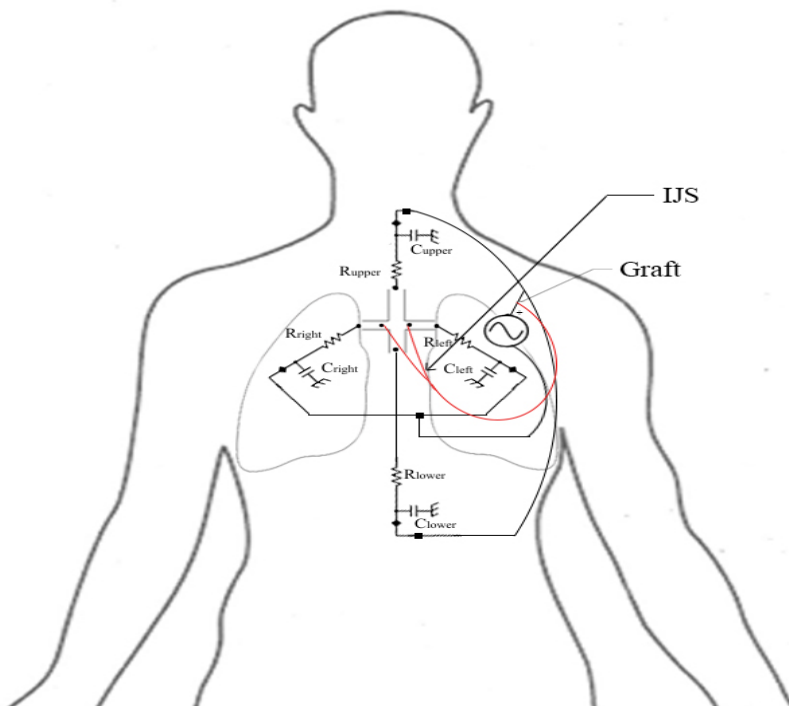


**Figure 3.2: Lumped Parameter model of proposed self powered Fontan Procedure**



## Pump

The MFL will be driven by a Harvard Apparatus pulsatile pump, see Fig. 4. The MFL will be operated using water instead of blood, therefore, it is important to matching non-dimensional parameters to ensure physiologically relevant behavior. The pulsatile pump allows for the adjustment of three variables: output phase ratio, frequency or RPM, and stroke volume, that is, the volume of water ejected with each pulse. The proper tuning of these settings is done by matching two non-dimensional parameters, which describe the flow behavior, to those measured in patient physiology; namely, the Womersley number, denoted  $\alpha$ , and the Reynolds number, denoted  $Re$ , defined such that,

$$\alpha = \frac{D}{2} \sqrt{\frac{\rho \pi f}{\mu}} \quad (8)$$

$$Re = \frac{\rho v D}{\mu} \quad (9)$$



**Figure 3.3: Harvard Apparatus Large animal Pulsatile Pump**

It can be seen that the Womersley number and Reynolds number are functions of known physiological values. Therefore, these non-dimensional parameters for the target population can be determined using average physiological values from medical literature.

As the MFL models the upper systemic circulation, lower systemic circulation, left pulmonary circulation, and right pulmonary circulation, it is of interest to derive these non-dimensional parameters in the superior vena cava, inferior vena cava, left pulmonary arteries and right pulmonary arteries. These values have been calculated and tabulated below in Table 3.1.

**Table 3.1. Anatomically Derived Non-Dimensional Parameters**

Vasculature	Womersely Number	Reynolds Number
Superior Vena Cava	6.89	578.76
Inferior Vena Cava	6.89	1350.44
Left Pulmonary Artery	5.52	1085.9
Right Pulmonary Artery	5.52	1085.9

Given that the diameter of tubing used within the MFL is known, the pump frequency can be calculated from the Womersley number such that,

$$f = \frac{\mu}{\pi\rho} \left( \frac{2\alpha}{D} \right)^2 \quad (10)$$

Additionally, the Reynolds number dictates flow velocity based upon the geometry of the MFL. This flow velocity can be found such that,

$$v = \frac{\mu}{\rho D} Re \quad (11)$$

Knowing that the volumetric flow rate is a function of the velocity and flow cross-section, the flow rate that must be supplied by the pulsatile pump can be calculated such that,

$$Q = vA \quad (12)$$

The frequency and volumetric flow rate for each lump of the MFL has been calculated and tabulated below in Table 3.2.

**Table 3.2. Anatomically Derived Frequency and Individual Volumetric Flow Rate**

Vasculature	Frequency (cycle/min)	Volumetric Flow Rate (LPM)
Superior Vena Cava	22.4849	0.3464
Inferior Vena Cava	22.4849	0.8082
Left Pulmonary Artery	14.4321	0.5773
Right Pulmonary Artery	14.4321	0.5773

Recall that the superior systemic circulation is parallel to the inferior systemic circulation and the left pulmonary circulation is parallel to the right pulmonary circulation. Therefore the volumetric flow rate required of the pump is the sum of the upper and lower systemic circulations or the sum of the right and left pulmonary circulations. Also, notice that the resulting frequency in the systemic circulation (22.4849 cycle/min) is different than that in the pulmonary circulation (14.4321 cycle/min), therefore an average between these values will be selected to set the frequency (RPM) of the pump. Given that the Womersley number governs the frequency of the pump, the stroke volume is then adjusted such that the appropriate volumetric flow rate is achieved, as the flow rate is simply the algebraic product of frequency and stroke volume.

The output phase ratio for the pump is set such that the duration of the pump output matches the duration of systole in the cardiac cycle.

### Vascular Compliance

In modeling the vascular compliance of the infant anatomy, the MFL defined in [47] was simplified by bundling appropriate compliances values in order to match the flow loop geometry specified in the experiment. This is summarized in Table 3.3.

Due to the relative similarity between the IJS Fontan Mock Flow Loop used in this experiment and the reduced lumped parameter network model utilized in [25], all but the lower systemic compliance could be carried over.

**Table 3.3. Compliances for body surface area (BSA) of 0.67 m<sup>2</sup> and 1.2 m<sup>2</sup>**

BSA:	0.67 m <sup>2</sup>	1.2 m <sup>2</sup>
C <sub>ub</sub>	2.15 ± 0.06	3.12 ± 0.03
C <sub>liver</sub>	2.17 ± 0.07	4.41 ± 0.14
C <sub>lb</sub>	1.32 ± 0.013	3.86 ± 0.06
C <sub>rl</sub>	(0.69+0.88/4) ± 0.03	(1.70 + 1.76/4) ± 0.066
C <sub>ll</sub>	(0.69+0.88/4) ± 0.03	(1.70 + 1.76/4) ± 0.066
C <sub>tcpc</sub>	0	0
C <sub>ivc</sub>	(0.458+0.88/2) ± 0.03	(0.92 + 1.76/2) ± 0.055

In order to calculate the lower systemic compliance, the liver compliance and lower body compliance are combined such that,

$$C_{\text{lower}} = \left( \frac{1}{C_{\text{lb}}} + \frac{1}{C_{\text{liver}}} \right)^{-1} + C_{\text{ivc}} \quad (13)$$

Therefore, the resulting compliance values used in this experiment are given below in Table 3.4.

**Table 3.4. Vascular Compliance Utilized in Experiment**

Vascular Branch	Vascular Compliance (mL/mmHg)
C <sub>upper</sub> , Upper Systemic Compliance	3.12
C <sub>lower</sub> , Lower Systemic Compliance	3.86
C <sub>left</sub> , Left Pulmonary Compliance	2.14
C <sub>right</sub> , Right Pulmonary Compliance	2.14

With the values for vascular compliance identified, the compliance elements could be constructed in the fashion of a vertical flow accumulator. Traditionally, the function defining the vascular compliance in relation to volumetric flow rate is given such that,

$$Q(t) = \frac{d}{dt} \{C(t)[P(t) - P_{vg}(t)]\} \quad (14)$$

Therefore,

$$\Delta P(t) = \frac{1}{C} \int_{-\infty}^t Q(t) dt \quad (15)$$

and,

$$C(t) = \frac{V(t) - V_o}{\Delta P(t)} \quad (16)$$

In order to achieve the desired compliance value for the vascular compliance elements, the above equation can be modified to describe the compliance as a function of the compliance element geometry and fluid parameters.

$$C = \frac{\Delta V}{\Delta P} \quad (17)$$

$$C = \frac{\pi r_e^2 \Delta h}{\rho g \Delta h} \quad (18)$$

$$r_e = \sqrt{\frac{\rho g C}{\pi}} \quad (19)$$

Where  $r_e$  is the effective radius of the cylindrical compliance chamber. The resulting effective radii for the four compliance chambers are shown below in Table 3.5.

**Table 3.5. Required Effective Radius for Desired Compliance**

Vascular Branch	Effective Radius (in.)
$C_{\text{upper}}$ , Upper Systemic Compliance	0.3365
$C_{\text{lower}}$ , Lower Systemic Compliance	0.3742
$C_{\text{left}}$ , Left Pulmonary Compliance	0.2787
$C_{\text{right}}$ , Right Pulmonary Compliance	0.2787

The compliance chambers are constructed of Schedule 40 and Schedule 80 PVC pipe; therefore nominal pipe sizes are selected to most closely match the values required to produce the appropriate effective radius. In the case of the upper and lower compliance elements, an annular design approach was taken to accurately achieve the effective radius values.

### Vascular Resistance

In the MFL, the vascular resistance serves two purposes: first, to regulate the volumetric flow rate through branches of the loop and, second, to produce pressure losses across a lump similar to those observed in human cardiovascular physiology. According to medical literature, the upper systemic circulation receives approximately 30% of the total systemic blood flow while the lower systemic circulation receives approximately 70% of the total systemic blood flow. In the pulmonary circulation, the left and right branches each receive approximately 50% of the pulmonary blood flow. Thus, the vascular resistances are initially adjusted, or tuned, to control the ratio of flow within two parallel lumps of the flow loop.

Once the flow ratios had been met, the vascular resistances were varied in order to generate the appropriate pressure losses across each branch, while maintaining the

appropriate flow ratios. As the upper systemic branch is in parallel with the lower systemic branch, the change in pressure should be equivalent across both branches and is equal to the pressure loss across the entire systemic circulation. The same applies to the left and right pulmonary branches and the total pulmonary pressure loss. The desired changes in pressure are tabulated below in Table 3.6.

**Table 3.6. Pressure Drop to be observed across Systemic and Pulmonary Circulations**

Vasculature	Pressure Drop (mmHg)
Systemic Circulation	53
Pulmonary Circulation	10

### **Injection Jet Shunt Prototyping**

For the IJS, three prototypes were produced with varying internal diameters: 2mm, 3mm and 4mm. These were designed to introduce an entrainment jet concentric to the flow within the pulmonary artery to which the IJS is grafted. It is theorized that the entrainment jet will exchange momentum with the flow in the pulmonary arteries, with the hope that this will result in a decrease of the localized vascular resistance at the TCPC and therefore decrease the pressure at the IVC. It can be seen in the IJS schematic in Fig. 5 that the diameter increases at the point of entrainment. This is because a small tube is built into the IJS to ensure concentricity of the jet flow. Therefore, to isolate the effects of the momentum imparted by the jet stream, the diameter of the vasculature was increased around the internal tube such that the flow cross sectional area remains constant. The IJS prototypes were 3D-printed, as this provided the best method for the precision manufacturing necessary for the geometry. After printing, the IJS were sanded and coated with a water-proof sealant to prevent any leaking.

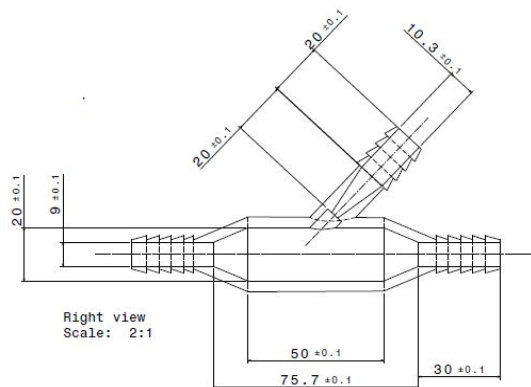


**Figure 3.4: 2D draft of CAD model of IJS**

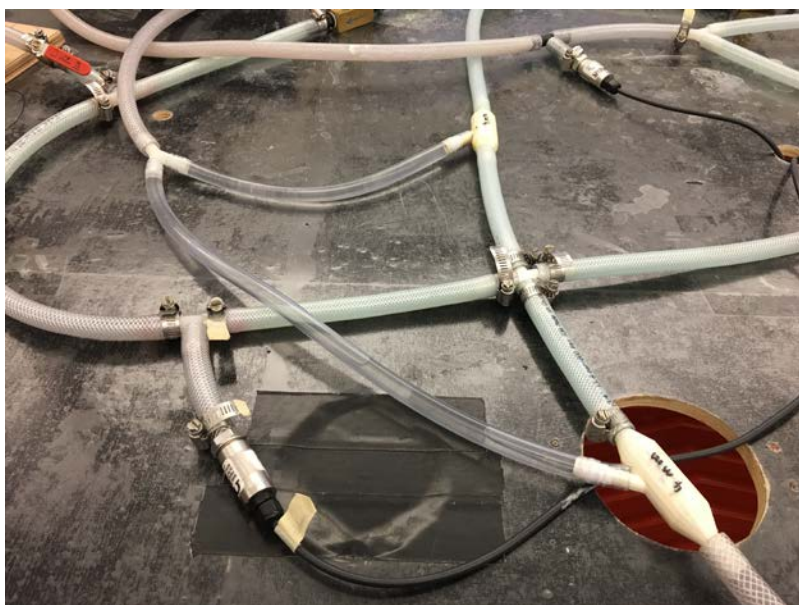


**Figure 3.5: Figure showing the placement of IJS in TCPC section**



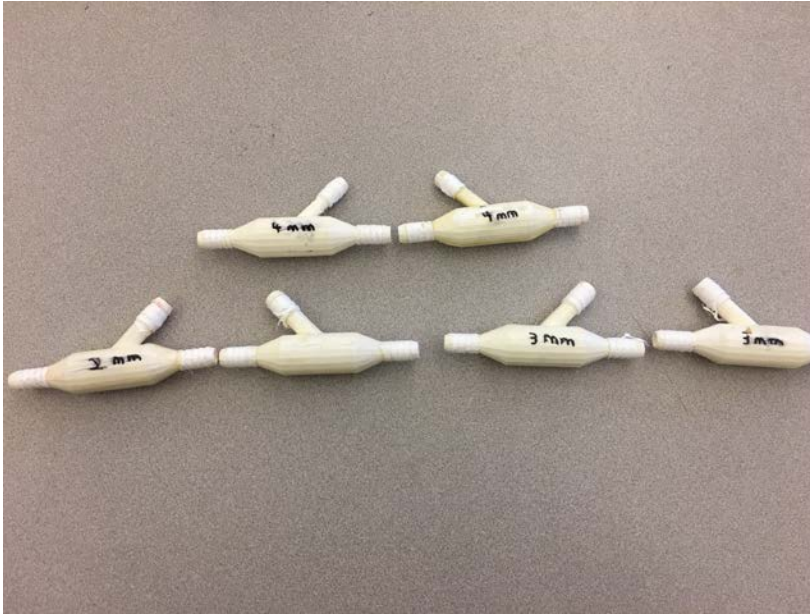


**Figure 3.6: Figure showcasing different prototypes of IJS**

## **Chapter IV**

### **Experimentation**

#### **Components**

##### **Test Rig/Table Top**

The table top is an integral part of the whole MFL setup as it holds each and every component of the loop at its proper location. This table top is a sturdy frame based structure and made of pine wood. Many holes have been drilled at various locations on this table top for clamping and mounting the sensors, tubing and chambers and also allowing the system to have proper spill drainage and wire harnessing.

##### **Harvard Apparatus Pump**

This is a pulsatile pump which simulates the pumping action of the heart for large animals. It contains heart type ball valves which are made of silicone rubber. The flow across these ball valves is very smooth. In this pump design, only materials like silicone rubber, acrylic plastic, and PTFE come in contact with the fluid as a result there is a minimal chance of hemolysis. It has a mechanically actuated piston which moves back and forth in a transparent cylinder head. In this mechanism, the piston travels to the farthest end of the cylinder irrespective of the selected stroke volume. This insures that the fluid is completely emptied from the cylinder at each stroke. The RPM decal determines the frequency of the stroke rate of the piston for a set stroke value and the Output to Input phase ratio determine the amount of systole ratio should be present in a whole cardiac cycle produced by the pump for a particular Stroke and RPM setting.

**Compliance chamber:**

The compliance chambers are made of schedule 40 and schedule 80 PVC pipe. A compliance chamber is placed in each of the four compartments of the loop, i.e. upper and lower systemic circulation and right and left pulmonary circulation, to mimic the compliance offered by that section.



**Figure 4.1: Figure showing a compliance chamber installed in the MFL**

**Resistors**

Needle valves have been used as a resistor to incorporate resistance in each section of MFL. These are made up of Stainless steel with  $\frac{1}{2}$ " inch NPT Female thread size. It has a very accurate flow rate range which lies between 0-22.5 (GPM) and the pressure range from 0-5000 PSI with cracking pressure of 1-2.5 (PSI).



**Figure 4.2: The figure showing the resistor installed in the MFL**

### **Flow Meters**

A flow meter is placed in every compartment of the flow loop to measure the flow rate provided by that section. These flow meters work on turbine based principle and mainly applicable for low flow rate applications. The turbine technology provides a high accuracy for flow rate applications. Due to the smaller diameter, the inertia of the turbine is very low hence this sensor reacts quickly to on/off dispensing applications. This sensor can measure the flow rate from 0.1 to 2.5 LPM.

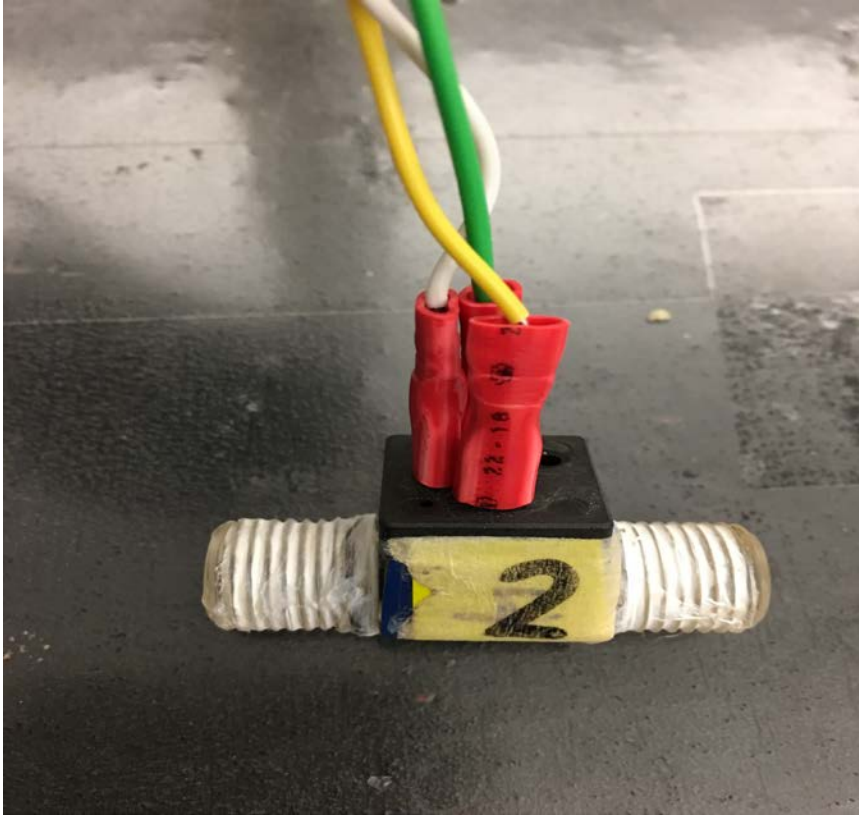


**Figure 4.3: The figure showing a flow meter installed in the MFL**

### **Pressure Sensors**

These are very precise and robust analog pressure sensors. In total there are four pressure sensors installed in the whole MFL. One is installed in the Aortic flow line, i.e. the line connecting the pump to the bifurcation of the systemic circulation, and another two are placed in upper and lower part of the systemic circulation. The last one is placed in the venous flow line, i.e. the line returning from the pulmonary circuit to the reservoir. These sensors can read any pressure of the range 0-15 PSIG and generates 0-100 mV



respectively.



**Figure 4.4: The figure showing a pressure sensor installed in the MFL:**

#### **Tubing**

To mimic the whole vasculature of the body a ½ inch inner diameter hose is used throughout the MFL. This hose is made of clear braided PVC reinforced materials.

**Figure 4.4: The figure showing a pressure sensor installed in the MFL:**

#### **Data Acquisition System (DAQ)**

To acquire all the signals from these sensors (flow meters and Pressure sensor) a Data Acquisition module of national Instrument is used. This is a modular chassis based

data acquisition system with eight slots to input different modules of Analog and Digital sensor readers. There are three major components of this system:

### **cDAQ chassis**

The cDAQ-9174 is a 4-slot CompactDAQ USB chassis designed for small, portable, mixed-measurement test systems. Combine the cDAQ-9174 with up to four NI C Series I/O modules for a custom analog input, analog output, digital I/O, and counter/timer measurement system. Out of these four slots only two are used by a digital module NI 9361 and another one is an analog module, i.e. NI 9205. One Compact DAQ system combines sensor measurements with voltage, current, and digital signals to create custom, mixed-measurement systems with a single, simple USB cable back to the PC, laptop, or netbook. The cDAQ-9174 has four 32-bit general-purpose counter/timers built in. These counters can be accessed through an installed, hardware-timed digital NI C Series module such as the NI 9401 or NI 9402 for applications that involve quadrature encoders, PWM, event counting, pulse train generation, and period or frequency measurement.

### **Digital module**

This digital module- NI 9361 is being used to log data sent by each of the flowmeters. This module is an 8-channel differential or single-ended counter input module for Compact DAQ. Each channel is configured to read a single pulse train or combine them to read up to four incremental encoders. Sensors can be directly connected with open-collector or push-pull outputs. It has eight flexible, 32-bit counters where each counter is capable of standard counter measurements such as edge counting, pulse width,

period, and frequency measurements. In addition, the counters can perform encoder position and velocity measurements. The NI 9361 counters provide enhanced frequency and duty-cycle (PWM) measurements. The counters support a dynamic averaging mode, so you can obtain frequency measurements that are optimized for accuracy and latency from 0 Hz up to high rates. For duty-cycle measurements, the counters can correctly measure over the full range from 0 percent to 100 percent. As the flow meters are turbine based, a pulse train is generated when it sees the flow. Therefore the frequency measurement output was selected and then by configuring the sample size, and buffer size parameter in this module the frequency of the pulse train is obtained.

### **Analog Module**

The National Instruments 9205 is a C Series module, for use with NI CompactDAQ and CompactRIO chassis. The NI 9205 features 32 single-ended or 16 differential analog inputs, 16-bit resolution, and a maximum sampling rate of 250 kS/s. Each channel has programmable input ranges of  $\pm 200\text{mV}$ ,  $\pm 1$ ,  $\pm 5$ , and  $10\text{V}$ . There are two connector options for the NI 9205; a 36-position spring terminal connector for direct connectivity or a 37-position D-Sub connector. As a result, this module is used to acquire the voltage signal sent by each of the pressure sensors.

### **Software**

A code is written in Labview software to plot the raw data, i.e. frequency and voltage values acquired from the flow meters and pressure sensor respectively on real time basis. Then these raw data values were logged in an excel spread sheet format. After



that, a Matlab script was developed to do the post processing on these logged data to obtain the flow rate values and pressure values.

### **Calibration of Flowmeters**

At first, the pump is set to produce a specific output. The flowmeter which has to be calibrated is placed in line to the line connecting the pump and graduated reservoir. Now, the time taken by water to fill a specific volume level in the graduated reservoir is obtained by using a chronometer. Hence the flow rate of the system is calculated from this “Time duration” and “Volume”. For the same volume, the frequency values generated by these flowmeter are logged in an excel spread sheet in the workstation using Labview code. Now, the flowrate and frequency values are logged into another excel spread sheet and plotted against each other. A linear curve fit technique was used to find the calibration equation for that particular flowmeter for a good R<sup>2</sup> value. The same experiment was conducted with four different volume levels and for three different pump settings.

### **Calibration of Pressure Sensor**

Calibration equation of the pressure sensor was obtained from the data sheet provided by the company.

### **Process**

The pulsatile pump is set such that an output of 1.2 liter per minute (lpm) is produced; this requires pump settings of 40 RPM and 30 cubic centimeters (cc) per

stroke. The output phase ratio is set to 35 percent in order to match the ratio of systole to the entire heart cycle. The resistors are tuned in such a way that the 30% of the total systemic flow diversion towards the upper circulation and 70% of the total systemic flow diversion towards the lower circulation of the body. The ratio of pulmonary flow to systemic flow is one. Also, the return flow is equally split between both the right and left pulmonary circuit. The flow coming out of the pulmonary circuit directly goes back to the tank through the venous return line.

The flow rates and pressure values are logged using a National Instruments Data Acquisition System. This constitutes the baseline data set, as the flow loop geometry represents the typical Fontan circulation anatomy.

Then the IJS is added to the flow loop, which generated a parallel circuit that bypasses the systemic circulation. Additionally, a gate valve is attached at the distal end of the graft from the TCPC section, which simulates the total resistance provided by the graft. Again, the flow loop is run and data is recorded with the IJS and the gate valve fully open. Then, gradually, the gate valve is closed until the effective resistance provided by the graft is replicated. Pictures detailing the MFL setup are presented in Figures 6 through 8. In essence, this will output varying pressures and flowrates with the different shunts.

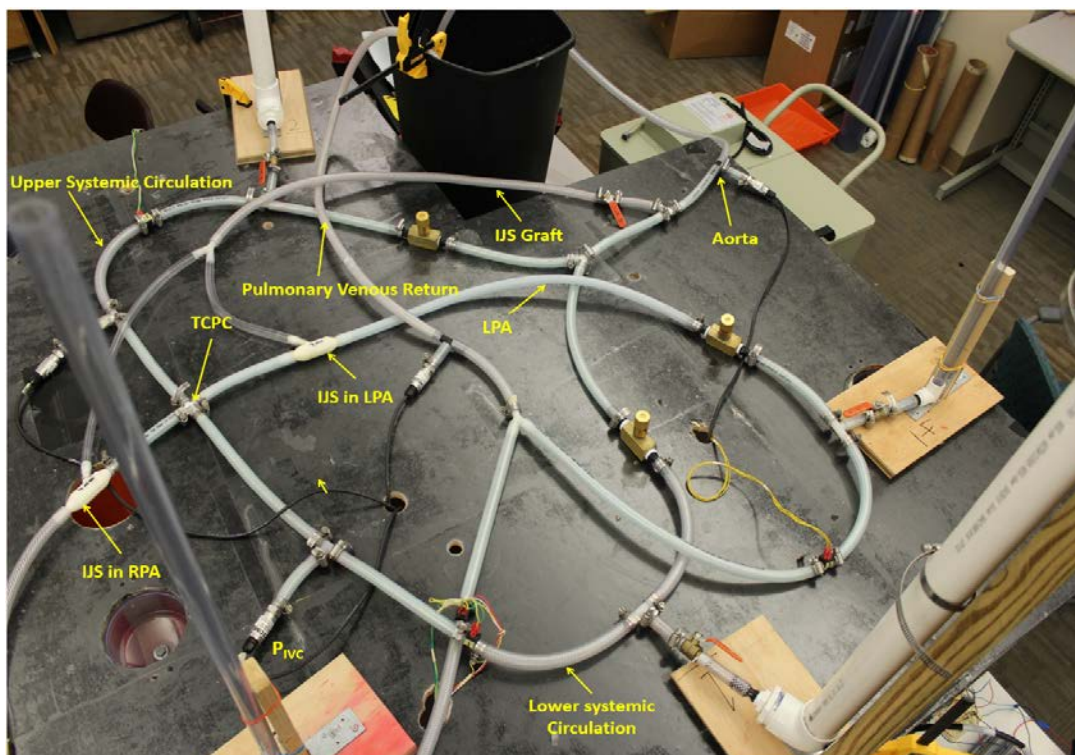


**Figure 4.5: A labelled figure of the complete MFL showing the elements of lumped parameter**

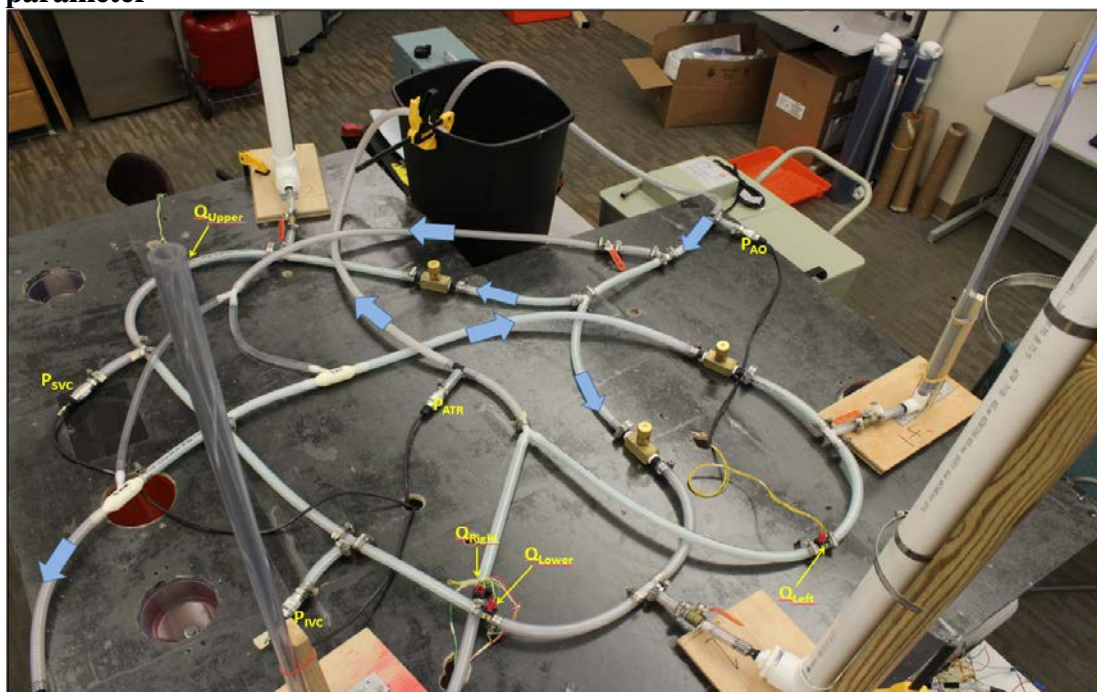


**Figure 4.5: A labelled figure showing the position of sensors and the flow directions in the MFL**

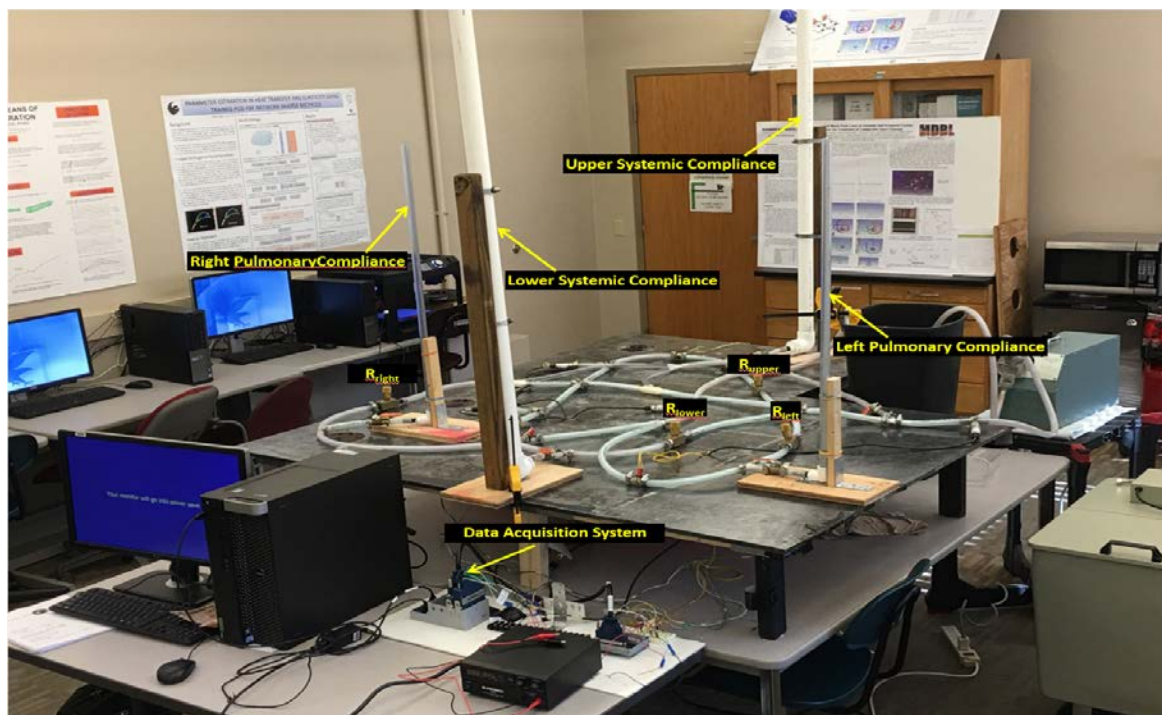


**Figure 4.5:** A labelled figure showing the position of compliance chambers and resistors in the MFL.

## Chapter V

### Results

The resulting flow characteristics for the baseline case as well as those produced by the partially closed and fully open IJS inlet cannula are tabulated in this section. The baseline configuration replicates the physiological flow and pressure values for the failing Fontan circulation case. The cardiac output is 1.24lpm while maintaining the 30% of the total systemic flow diversion towards the upper circulation and 70% of the total systemic flow diversion towards the lower circulation of the body. The ratio of pulmonary flow to systemic flow is one. Also, the return flow is equally split between both the right and left pulmonary circuit. The obtained aortic and caval pressures are analogous to the values of a failing Fontan circulation. Then by introducing different diameter IJS into the mock flow loop with the gate valve fully open, that is, in “Fully open Inlet cannula” configuration, the ratio of pulmonary flow ( $Q_p$ ) to systemic flow ( $Q_s$ ) increases to the range of 2.09-3.89 achieving an IVC pressure reduction of up to 4.94mmHg with respect to the Baseline case. Then in the “Partially closed Inlet cannula” configuration, the ratio  $Q_p/Q_s$  is reduced to the range 1.6-1.78 while the IVC pressure is reduced by as much as 5.86mmHg with respect to the Baseline case. The summary of the results is presented below in Table 5.1.

**Table 5.1. Results of Experiment**

	Fully Open IJS Inlet Cannula				Partially Closed IJS Inlet Cannula		
	Baseline	2mm IJS	3mm IJS	4mm IJS	2mm IJS	3mm IJS	4mm IJS
Cardiac Ejection (lpm)	1.24	1.099	1.125	1.169	1.017	1.0361	1.0362
$Q_U/Q_S$ (%)	30	29.12	34.75	37.47	33	29.35	31.34
$Q_L/Q_S$ (%)	70	70.88	65.25	62.53	67	70.64	68.66
$Q_{RP}/Q_P$ (%)	49.53	47.23	46.66	45.19	45	45.9	41.42
$Q_{LP}/Q_P$ (%)	50.47	52.77	53.34	54.81	55	54.1	58.58
$Q_P/Q_S$	<b>1</b>	<b>2.09</b>	<b>3.05</b>	<b>3.89</b>	<b>1.62</b>	<b>1.66</b>	<b>1.78</b>
$P_{AO}$ (mmHg)	75.7	32.22	27.34	24.51	39.22	37	36.66
$P_{IVC}$ (mmHg)	<b>20.48</b>	<b>15.54</b>	<b>16.57</b>	<b>17.53</b>	<b>15.12</b>	<b>15.1</b>	<b>14.62</b>
$P_{SVC}$ (mmHg)	20.2	15.12	16.02	17.07	14.7	14.67	14.19
$P_{ATR}$ (mmHg)	3.257	1.13	1.248	2.084	0.889	0.801	0.79

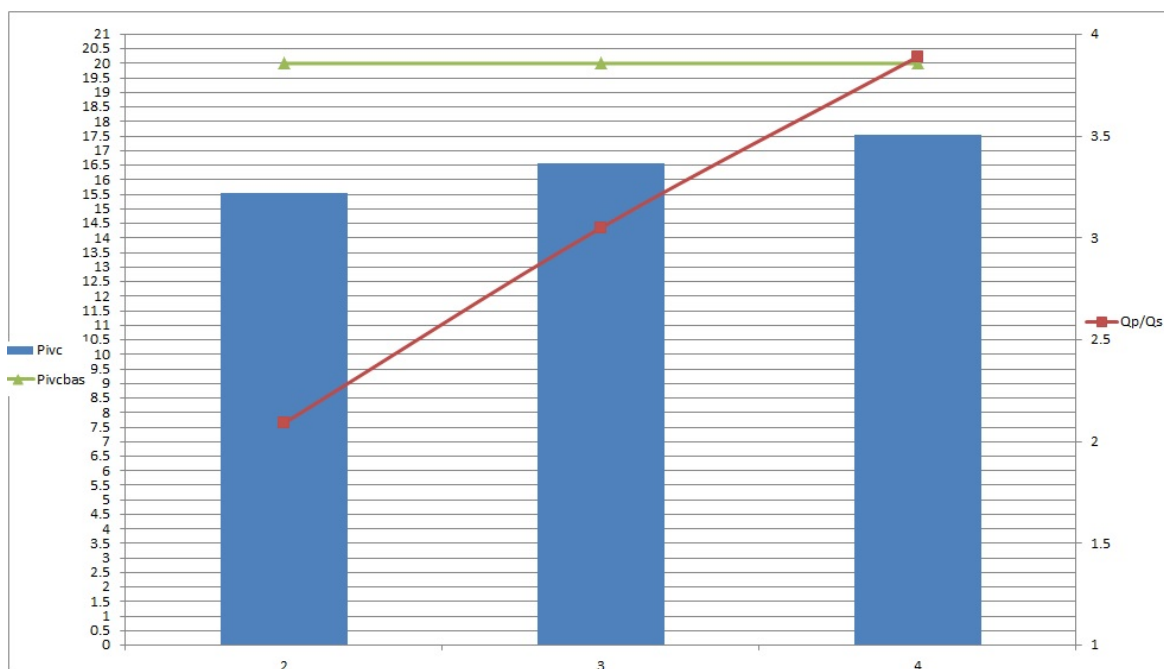


**Figure 5.1: Figure showing the Pressure values at IVC for baseline model and Pressure at IVC and  $Q_p/Q_s$  ratio for different diameter Jet shunt when the inlet cannula is fully open**



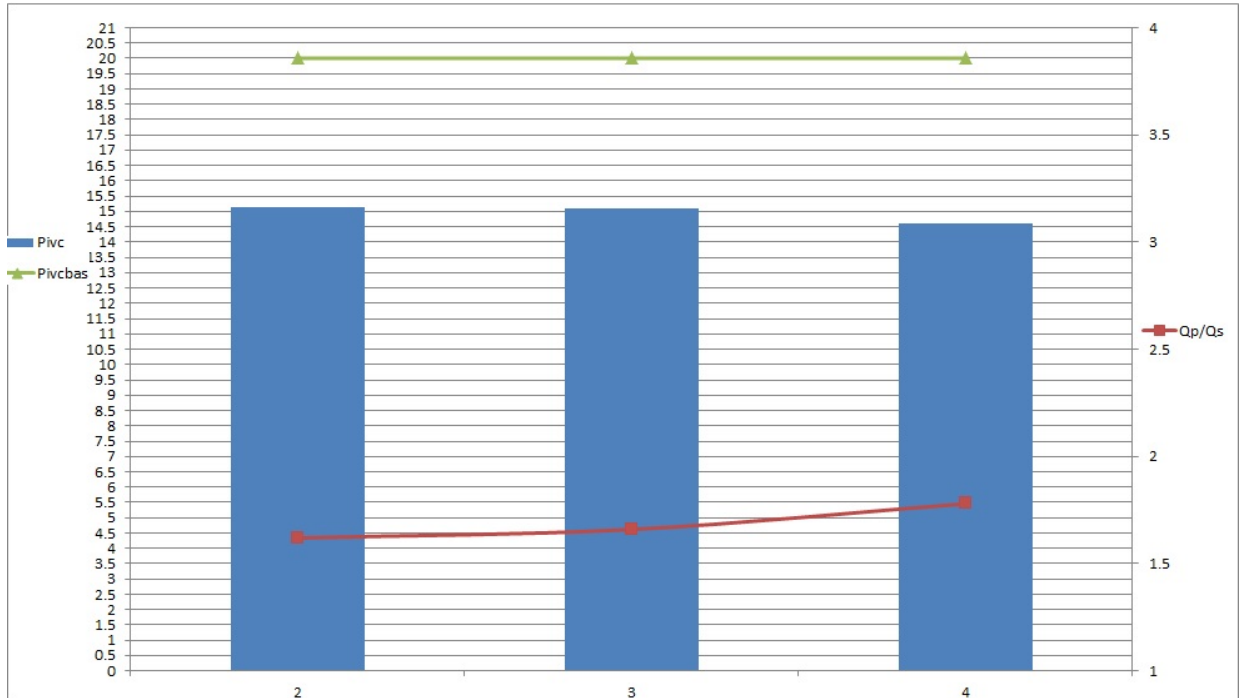


**Figure 5.2: Figure showing the Pressure values at IVC for baseline model and Pressure at IVC and Qp/Qs ratio for different diameter Jet shunt when the inlet cannula is partially closed**

### Baseline case

Here flow rates and pressure plots for the baseline model has been showcased.

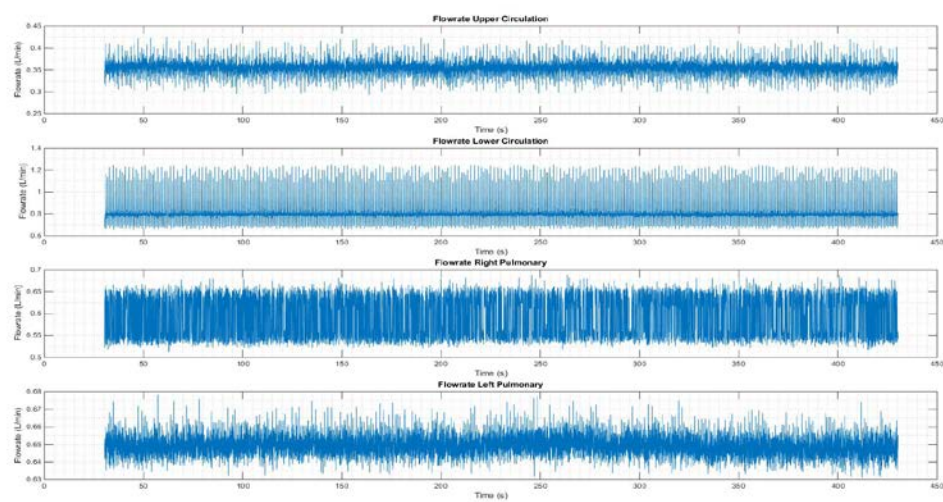


**Figure 5.3: Flow rates of baseline model (Top to Bottom) – Upper Circulation, Lower Circulation, Right Pulmonary Circulation and Left Pulmonary Circulation**

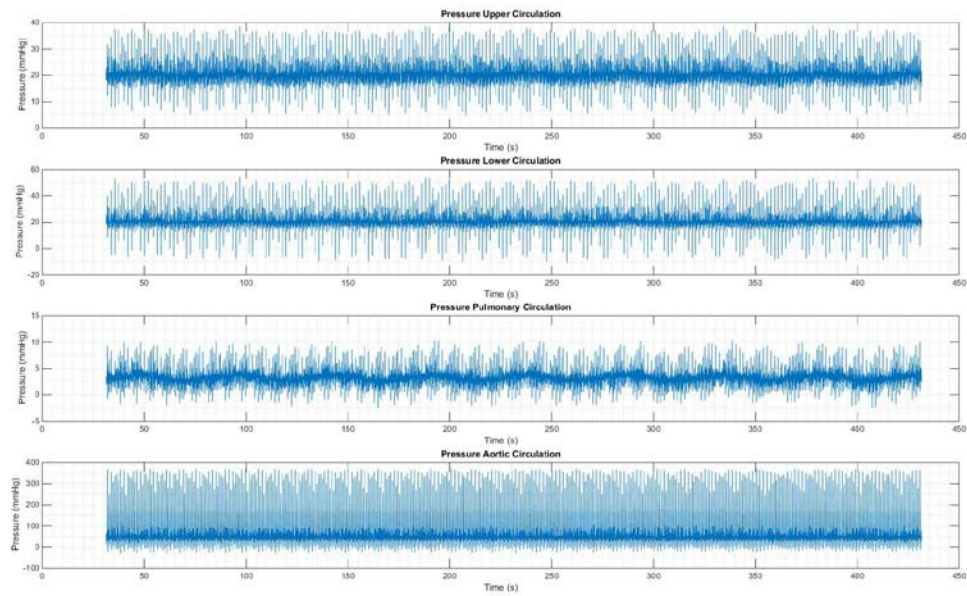


**Figure 5.4: Pressure Plot of baseline model (Top to Bottom) – Upper Circulation, Lower Circulation, Pulmonary Circulation and Aortic Circulation**

### With Fully Open IJS Inlet Cannula

#### Case 1: With 2mm IJS

In this case, the 2mm IJS was tested in the MFL while the inlet cannula was kept in fully open position.

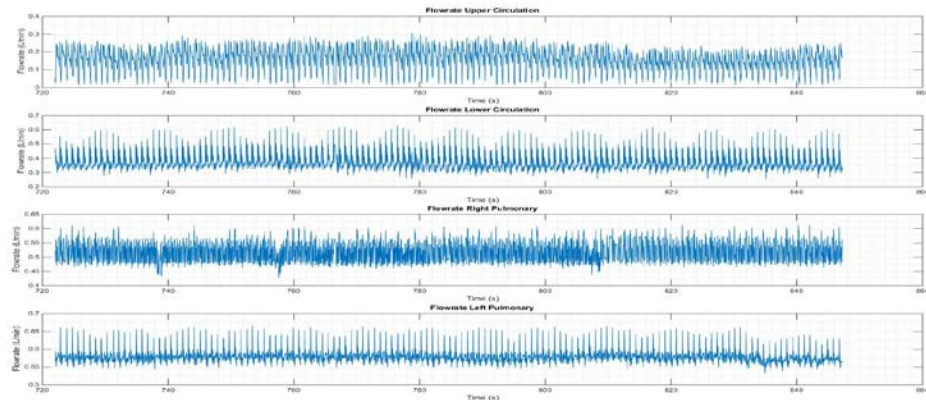


**Figure 5.5: Flow rate plot for 2mm IJS with fully open Inlet cannula (Top to Bottom) – Upper Circulation, Lower Circulation, Right Pulmonary Circulation and Left Pulmonary Circulation**



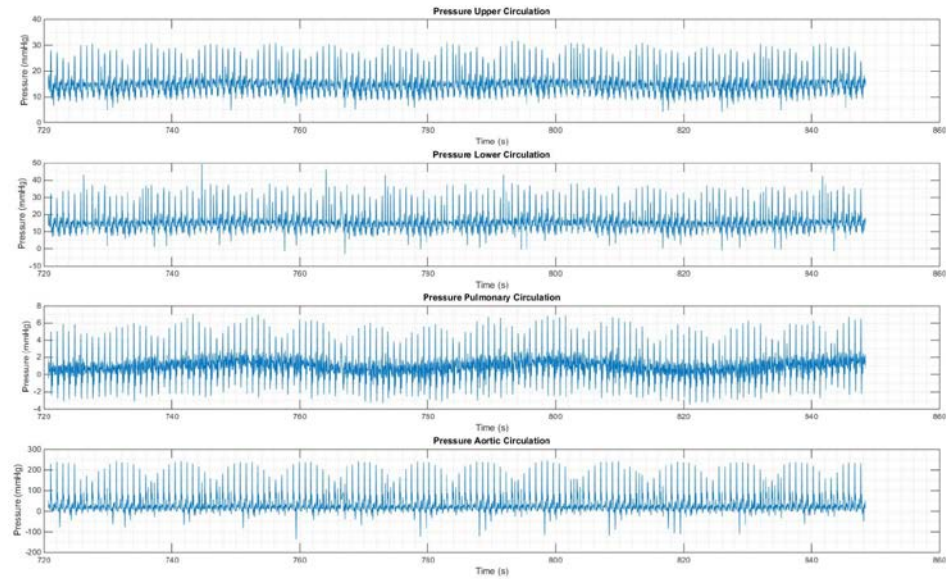


**Figure 5.6: Pressure Plot for 2mm IJS with fully open Inlet cannula (Top to Bottom) – Upper Circulation, Lower Circulation, Pulmonary Circulation and Aortic Circulation**

### With Partially Closed IJS Inlet Cannula

#### Case 1: With 2mm IJS

In this case, the 2mm IJS was tested in the MFL while the inlet cannula was kept in partially closed position

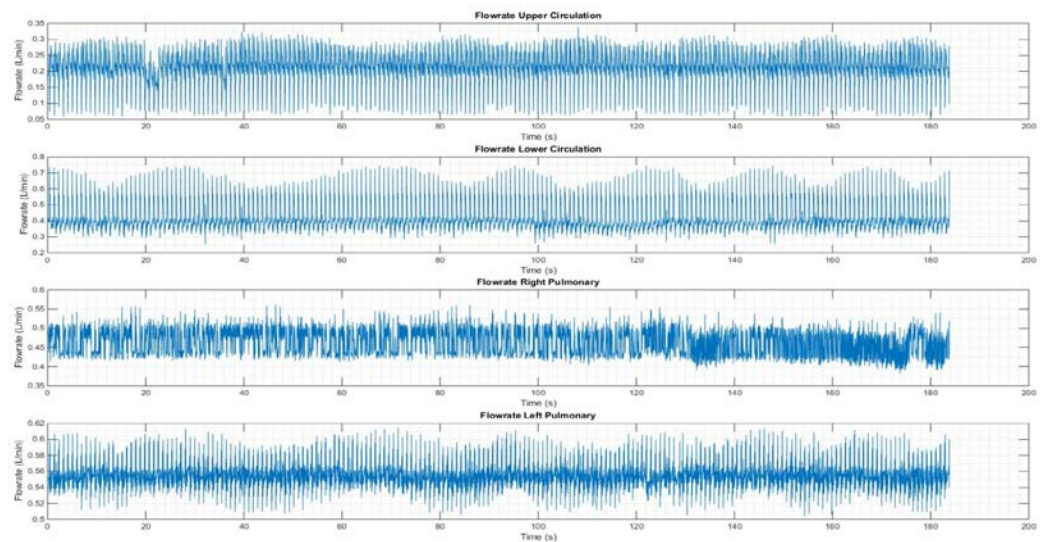


**Figure 5.7: Flow rate Plot for 2mm IJS partially open Inlet cannula Upper Circulation, Lower Circulation, Right Pulmonary Circulation and Left Pulmonary Circulation**

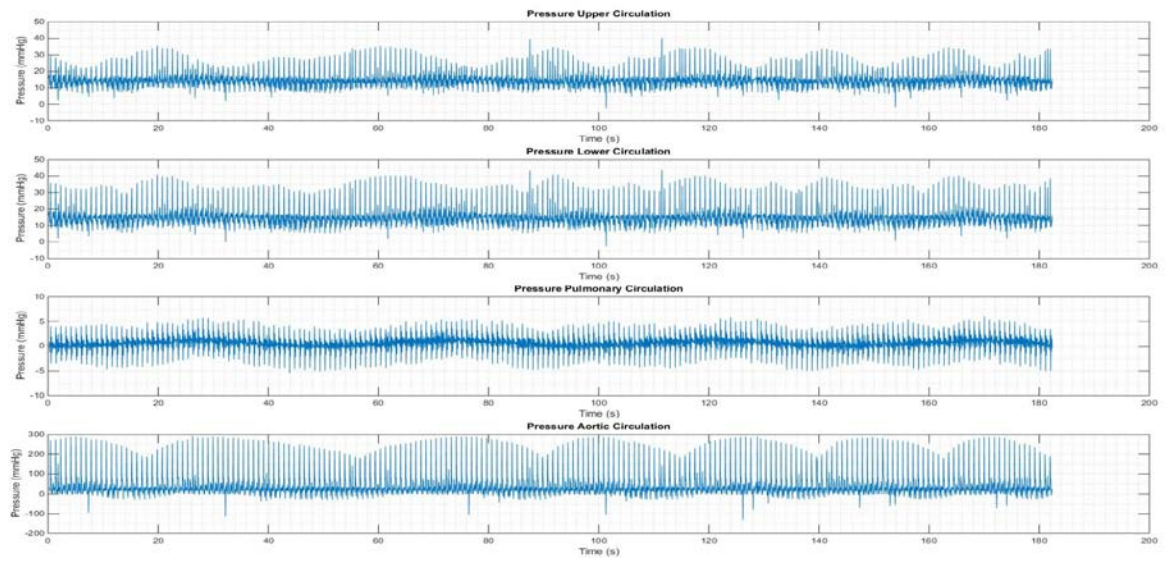


**Figure 5.8: Pressure Plot for 2mm IJS partially open Inlet cannula (Top to Bottom) – Upper Circulation, Lower Circulation, Pulmonary Circulation and Aortic Circulation.**

## Chapter VI

### Discussion, Conclusions, and Future Work

In this section we will elaborate on the results in detail along with the conclusion of this thesis. Future work for this project will also be discussed, and this will entail the future recommendation and modification to this experiment. Future work will also discuss how this experiment may be upgraded to the next level.

#### Discussion

It is observed that the increased IJS diameter results in a decreased resistance in the IJS graft, as the area reduction is less severe; hence yielding higher IJS flow rate and therefore higher  $Q_p/Q_s$  ratio. For the 2mm “fully open IJS inlet cannula” configuration, the IVC pressure reduction was 4.94mmHg yielding a  $Q_p/Q_s$  ratio of 2.09 while larger IJS (3mm and 4mm) produced less IVC pressure reductions at larger  $Q_p/Q_s$  ratios (up to 3.05). These values of IVC pressure reduction are promising, but they come at the expense of excessive IJS flow (and therefore excessive  $Q_p/Q_s$  ratios) which will in turn reduce the resulting systemic flow and, therefore, deprive the body of oxygenated blood.

#### Partially closure of Inlet cannula

In order to restrict the IJS flow and therefore limit the  $Q_p/Q_s$  ratio, the gate valve of the IJS valve is partially closed to achieve the maximum physiologically allowed  $Q_p/Q_s$  ratio of approximately 1.7. Partially closing the gate valve essentially simulates a steeper degree of implantation of the IJS graft in the Aorta or simply a smaller diameter graft. For

the 2mm “partially closed IJS inlet cannula” configuration, the IVC pressure reduction was 5.36mmHg yielding a  $Q_p/Q_s$  ratio of 1.62 while larger IJS (3mm and 4mm) gradually produced higher IVC pressure reductions at  $Q_p/Q_s$  ratios that did not exceed 1.8. This results clearly show the trend of how the IJS entrainment effect reduces the localized vascular resistance at the TCPC and lowers the resulting caval pressures

### **Conclusions**

A novel alternative to the Fontan circulation that includes a bifurcating graft, or Injection Jet Shunt (IJS), is experimentally tested. The IJS is used to “entrain” the pulmonary flow and thus provide assistance while reducing the caval pressure. A benchtop Mock Flow Loop (MFL) is configured to validate this hypothesis. The MFL is based on a Lumped-Parameter Model (LPM) of the Fontan circulation and is comprised of upper and lower systemic, as well as, left and right pulmonary compartments. Several IJS nozzle diameters are tested to validate the hypothesis and optimize the improvement. The inclusion of the IJS in the Fontan circulation is observed to indeed produce an entrainment effect that results in a reduction of the localized vascular resistance at the TCPC and therefore yielding the desired reduction of the caval pressure. However, the inclusion of the IJS in the MFL resulted in a reduction in cardiac ejection so the entire caval pressure reduction cannot be fully attributed to the entrainment effect. Future work will focus on the physiological response due to reduced cardiac ejection and systemic flow, such as increased cardiac function and decreased vasculature resistance, to simulate homeostatic reaction during the post-operative period.

**Future Work**

In future work, a method to account for change in pulmonary vascular resistance with the change in pulmonary flow rate will be incorporated in the MFL. A baroreceptor reflex setting will be added to the loop. The designs of IJS will be revised to make the insertion angle as shallow as possible. Also, instead of turbine based flow meters, magnetic flow meters will be installed in the loop, which will make the flow rate data very accurate. The LabView code will be modified in such a way that a separate post processing script will not be necessary.

## References

- [1] Fontan, F., and E. Baudet. "Surgical repair of tricuspid atresia." *Thorax* 26.3 (1971): 240-248.
- [2] Petrossian, E. D., et al. "Early results of the extracardiac conduit Fontan operation." *The Journal of thoracic and cardiovascular surgery* 117.4 (1999): 688-696.
- [3] Mondésert B, Marcotte F, Mongeon FP, Dore A, Mercier LA, Ibrahim R, Asgar A, Miro J, Poirier N, Khairy P. Fontan circulation: success or failure? *Can J Cardiol.* 2013;29(7):811-20.
- [4] Ovroutski S, Ewert P, Miera O, Alexi-Meskishvili V, Peters B, Hetzer R, Berger F. Long-term cardiopulmonary exercise capacity after modified Fontan operation. *Eur J Cardiothorac Surg.* 2010;37(1):204-9.
- [5] Caruthers RL, Kempa M, Loo A, Gulbransen E, Kelly E, Erickson SR, Hirsch JC, Schumacher KR, Stringer KA. Demographic characteristics and estimated prevalence of Fontan-associated plastic bronchitis. *Pediatr Cardiol.* 2013;34(2):256-61.
- [6] Rao PS. Protein-losing enteropathy following the Fontan operation. *J Invasive Cardiol.* 2007;19(10):447-8.
- [7] Khanna G, Bhalla S, Krishnamurthy R, Canter C. Extracardiac complications of the Fontan circuit. *Pediatr Radiol.* 2012;42(2):233-41.
- [9] Diller GP, Giardini A, Dimopoulos K, Gargiulo G, Müller J, Derrick G, Giannakoulas G, Khambadkone S, Lammers AE, Picchio FM, Gatzoulis MA, Hager A. Predictors of morbidity and mortality in contemporary Fontan patients: results from a multicenter study including cardiopulmonary exercise testing in 321 patients. *Eur Heart J.* 2010;31(24):3073-83.
- [10] Gentles TL, Gauvreau K, Mayer JE, Jr., Fishberger SB, Burnett J, Colan SD, Newburger JW, Wernovsky G. Functional outcome after the Fontan operation: factors influencing late morbidity. *J Thorac Cardiovasc Surg.* , 1997;114:392-403; discussion 404-5.
- [11] Deal BJ, Jacobs ML. Management of the failing Fontan circulation. *Heart.* 2012;98(14):1098-104..
- [12] Hebert A, Jensen AS, Idorn L, Sørensen KE, Søndergaard L. The effect of Bosentan on exercise capacity in Fontan patients; rationale and design for the TEMPO study. *BMC Cardiovasc Disord.* 2013;13:36.
- [13] Hraška V. Decompression of thoracic duct: new approach for the treatment of failing Fontan. *Ann Thorac Surg.* 2013;96(2):709-11.
- [14] Albal PG, Menon PG, Kowalski W, Undar A, Turkoz R, Pekkan K. Novel fenestration designs for controlled venous flow shunting in failing Fontans with systemic venous hypertension. *Artif Organs.* 2013;37(1):66-75.
- [15] Koçyıldırım E, Dur O, Soran O, Tüzün E, Miller MW, Housler GJ, Wearden PD, Fossum TW, Morell VO, Pekkan K. Pulsatile venous waveform quality in Fontan circulation-clinical implications, venous assists options and the future. *Anadolu Kardiyol Derg.* 2012;12(5):420-6..

- [16] Valdovinos J, Shkolyar E, Carman GP, Levi DS. In Vitro Evaluation of an External Compression Device for Fontan Mechanical Assistance. *Artif Organs*. 2013; available online ahead of print. [11]
- [17] Durham LA 3rd, Dearani JA, Burkhart HM, Joyce LD, Cetta F Jr, Cabalka AK, Phillips SD, Sundaeswaran K, Farrar D, Park SJ. Application of Computer Modeling in Systemic VAD Support of Failing Fontan Physiology. *World J Pediatr Congenit Heart Surg*. 2011;2(2):243-8.
- [18] Thacker D, Patel A, Dodds K, et al. Use of oral budesonide in the management of protein-losing enteropathy after the Fontan operation. *Ann Thorac Surg* ; 89:837-42, 2010.
- [19] Veldtman G, Webb G. Improved survival in Fontan-associated protein-losing enteropathy. *J Am Coll Cardiol* 64:63-64, 2014.
- [20] Throckmorton AL, Lopez-Isaza S, Downs EA, Chopski SG, Gangemi JJ, Moskowitz W. A viable therapeutic option: mechanical circulatory support of the failing Fontan physiology. *Pediatr Cardiol*. 2013;34(6):1357-65.
- [21] Giridharan GA, Koenig SC, Kennington J, Sobieski MA, Chen J, Frankel SH, Rodefeld MD. Performance evaluation of a pediatric viscous impeller pump for Fontan cavopulmonary assist. *J Thorac Cardiovasc Surg*. 2013;145(1):249-57.
- [22] Throckmorton AL, Ballman KK, Myers CD, Frankel SH, Brown JW, Rodefeld MD. Performance of a 3-bladed propeller pump to provide cavopulmonary assist in the failing Fontan circulation. *Ann Thorac Surg*. 2008;86(4):1343-7.
- [23] Rodefeld MD, Frankel SH, Giridharan GA. Cavopulmonary assist: (em)powering the univentricular fontan circulation. *Semin Thorac Cardiovasc Surg Pediatr Card Surg Annu*. 2011;14(1):45-54.
- [24] Strickland L. Kneass , *Practice and Theory of the Injector*, 1984, John Wiley & Sons, New York.
- [25] Pantalos, G. et al., Characterization of an adult mock circulation for testing Cardiac Support Devices. "ASAIO journal, 2004.
- [26] Verdonck,P.,et al., Mock loop testing of On-X Prosthetic mitral valve with Doppler echocardiography. *Artificial Organs*, 2002.
- [27] Naemura,K.,M Umezu, and T.Dohi, *Preliminary stuy on the New Self- closing Mechanical Mitral Valve* Artificial organs, 1999
- [28] Feng,Z.,et al., *In Vitro Hydrodynamic Characteristics Among Three Bileaflet Valve in the Mitral Position* Artificial organs, 2000
- [29] GrigioniM,et al., Hemodynamic Performance of small –Size Bileaflet Valves:Pressure Drop and Laser Doppler Anemometry Study of Three Prostheses. *Artificial Organs*, 2000
- [30] Walther,T., et al., *Experimental Evaluation and Early Clinical Results of a New Low-Profile Bileaflet Aortic Valve*. *Artificial Organs*, 2002.
- [31] Kolff, W., *Mock circulation to test pumps designed for permanent replacement of damaged hearts* .Cleveland clinicQuarterly, 1959.
- [32] Reul,H., *Hydromechanical simulation of systemic circulation*. Medical and biological engineering,1974
- [33] Rosenberg,G.,et al., *Design and evaluation of the Pennsylvania State University Mock Circulatory System*.ASAIO. 1981

- [34] Goodwin,J.,et al., *A model of educational simulation of infant cardiovascular physiology. Anesth Analg*,2004
- [35] Koenig,S.,et al., *Hemodynamic and pressure-volume responses to continuous and pulsatile ventricular assist in an adult mock circulation. ASAIO*,2004
- [36] Timms,D.,et al., *A complete mock circulation loop for the evaluation of left, right and biventricular assist devices. Artificial organs*, 2005
- [37] Bevegard, S., A Holmgren and B. Jonsson, *The effect of body position on the circulation at rest and during exercise, with special reference to the influence on the stroke volume. Acta Physiol Scand.*, 1960
- [38] Loh,M. and Y.Yu, *Feedback control design for an elastance-based mock circulatory system. American Control Conference*,2004.
- [39] Donovan ,F., *Design of a hydraulic analog of the circulatory system for evaluating artificial hearts. Artificial organs*,1975
- [40] Garrison,L.,et al., *A new mock circulatory loop and its application on the study of chemical additive and aortic pressure effects on hemolysis in the Penn State electric ventricular assist device. Artificial organs*,1994.
- [41] Woodruff ,S.,K.Sharp and G.Pantalos, *Compact compliance chamber design for the study of cardiac performance in microgravity. ASAIO*,1997
- [42] Bustmsnte, J., et al., *Physical model of the cardiovascular system. Dynasim 2003.*
- [43] Haft,J.,et al., *Design of an artificial lung compliance chamber for pulmonary replacement. ASAIO*,2003.
- [44] McMahon, T., et al., *Intra-aortic balloon experiments in a lumped-element hydraulic model of the circulation. J.Biomechanics*, 1971.
- [45] Stergiopulos N, Meister JJ, and W.N., *Evaluation of methods for estimation of total arterial compliance. Am J Physiol.*, 1995
- [46] Litwak, K., et al., *Ascending aorta outflow graft location and pulsatile ventricular assist provide optimal hemodynamic support in an adult mock circulation. Artificial organs*,2005
- [47] Vukicvic Marija,et al. "Mock circulatory system of the Fontan circulation to study respiration effects on venous flow behavior. "ASAIO journal (American society for Artificial Internal Organs: 1992) 59.3(2013):25



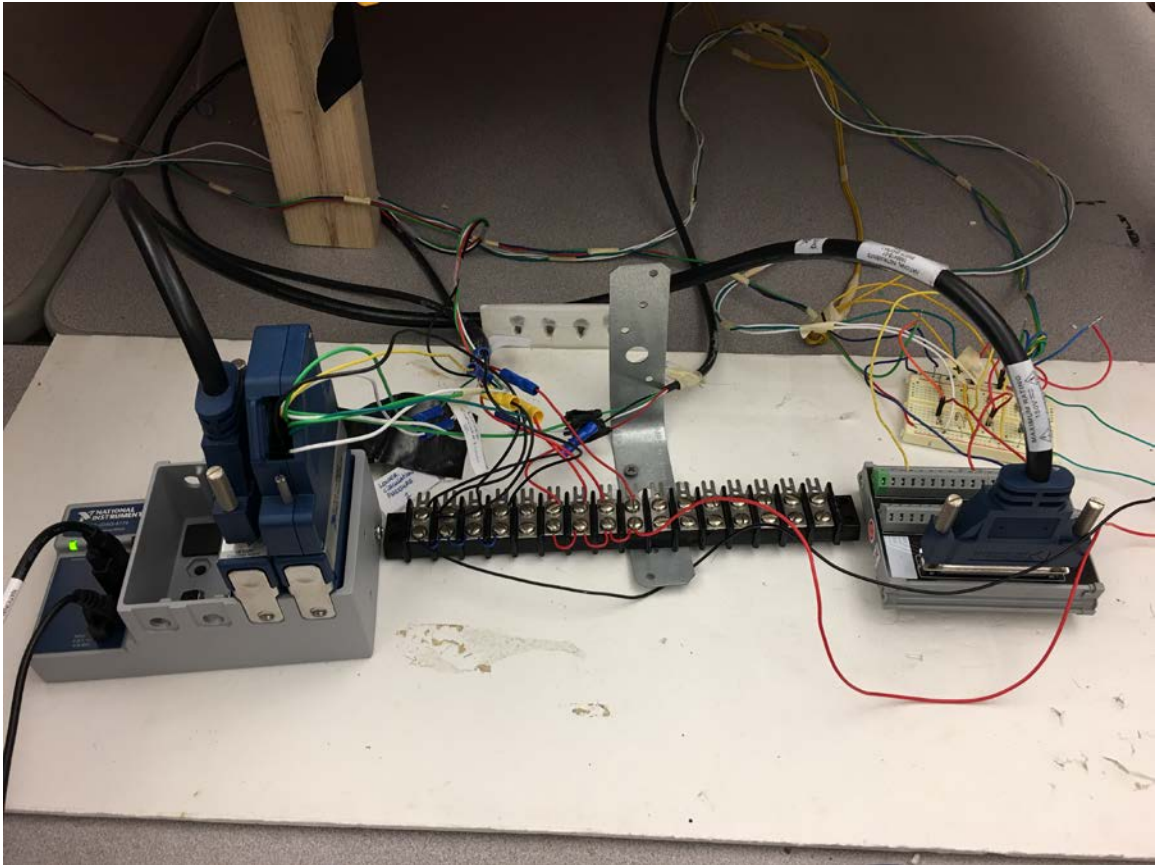
**Appendix B**

**Permission to Conduct Research**

[Insert permission form on this page.]

## Appendix C

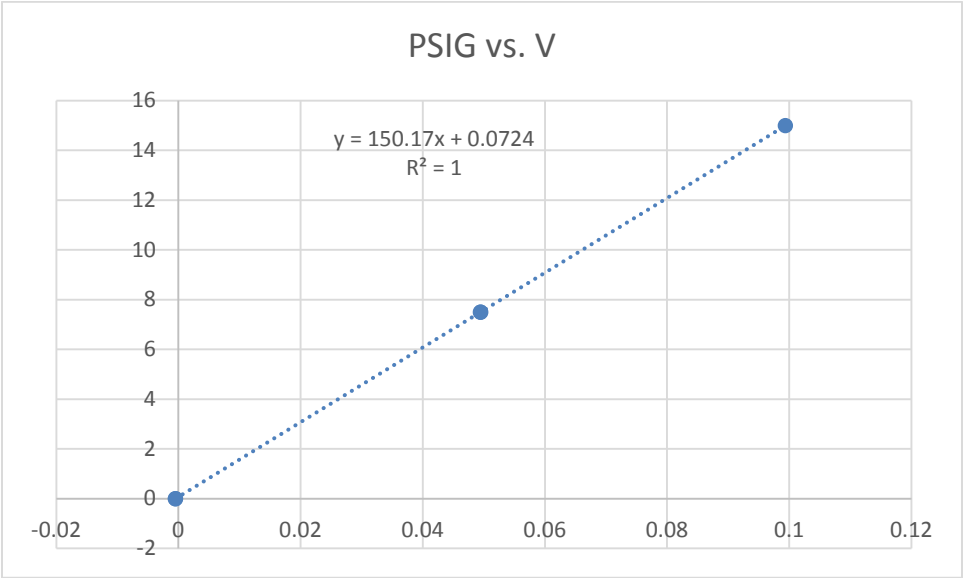
### Data Collection Device



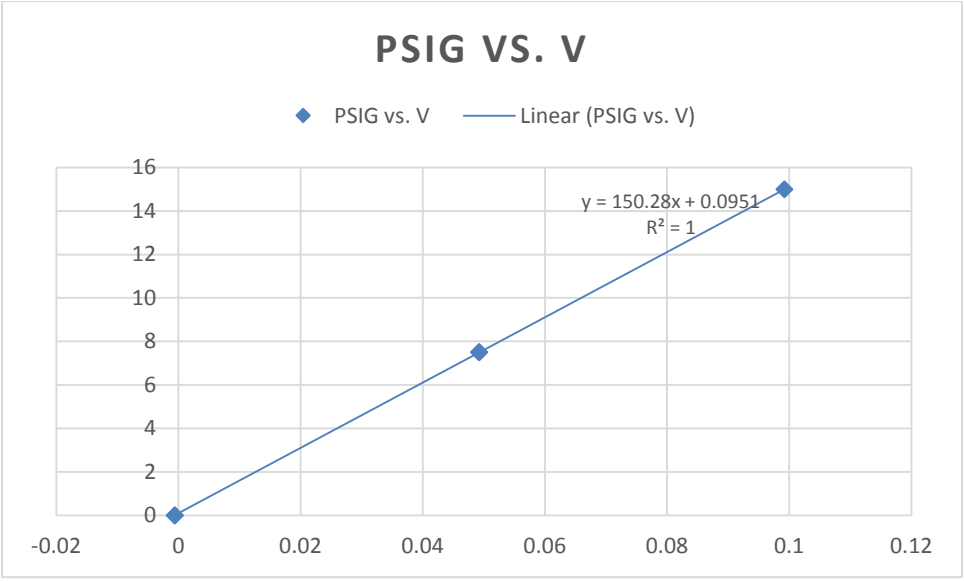
### Appendix D

#### Calibration Curves

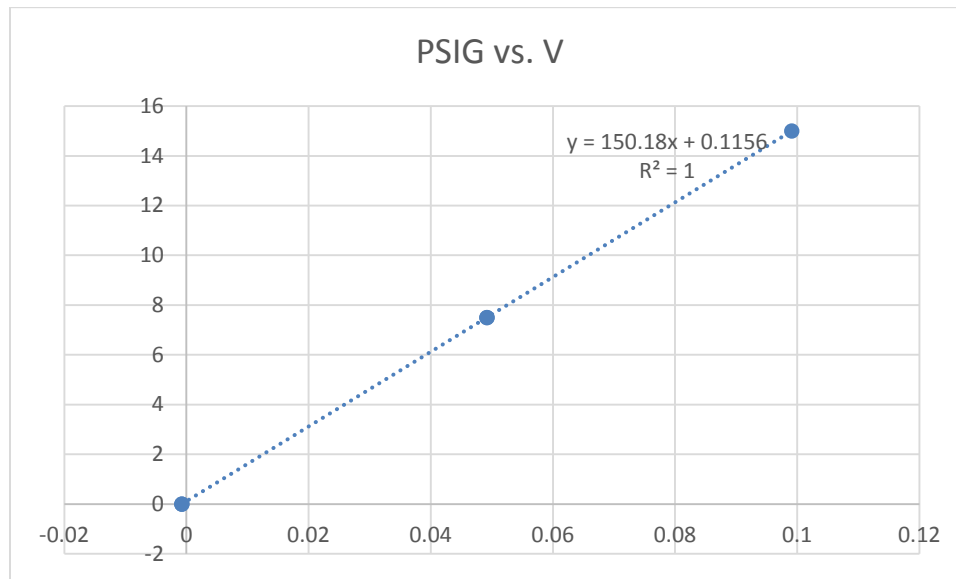
##### D2.1 Calibration curve of Pressure sensor in Upper Circulation



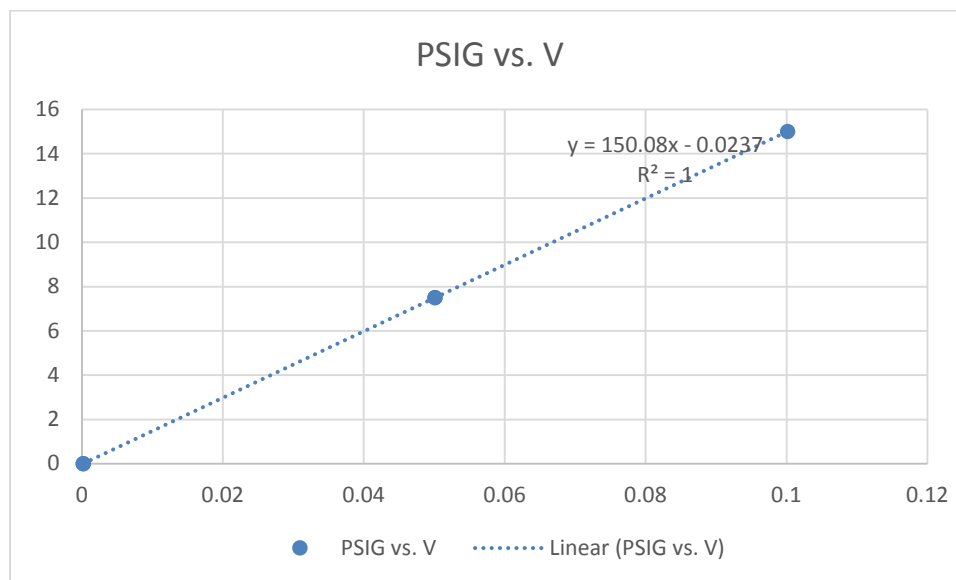
##### D2.2 Calibration curve of Pressure sensor in Lower Circulation



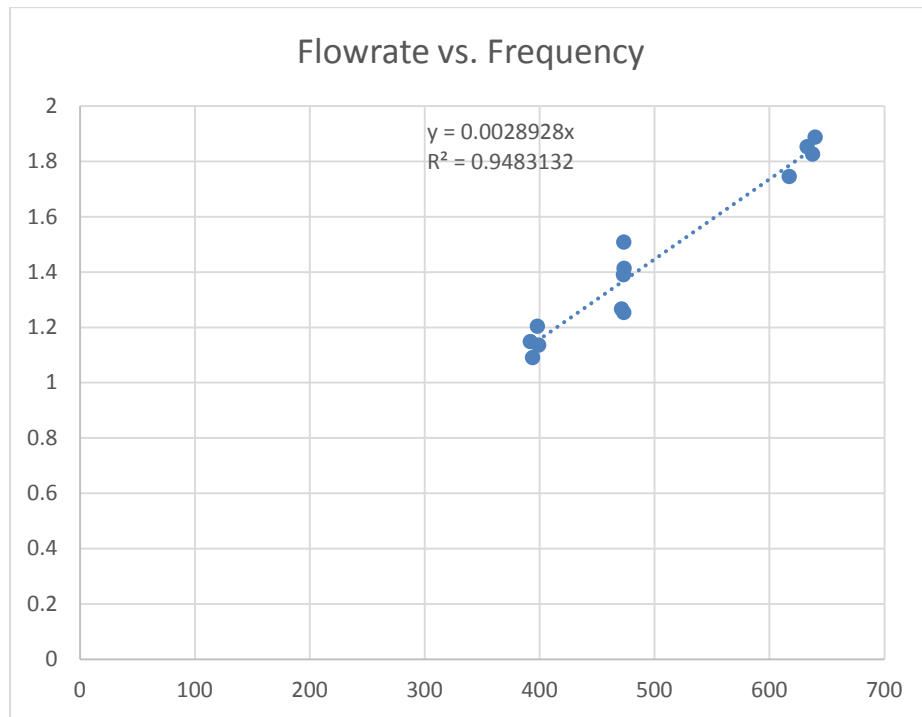
## D2.3 Calibration curve of Pressure sensor in Pulmonary Circulation



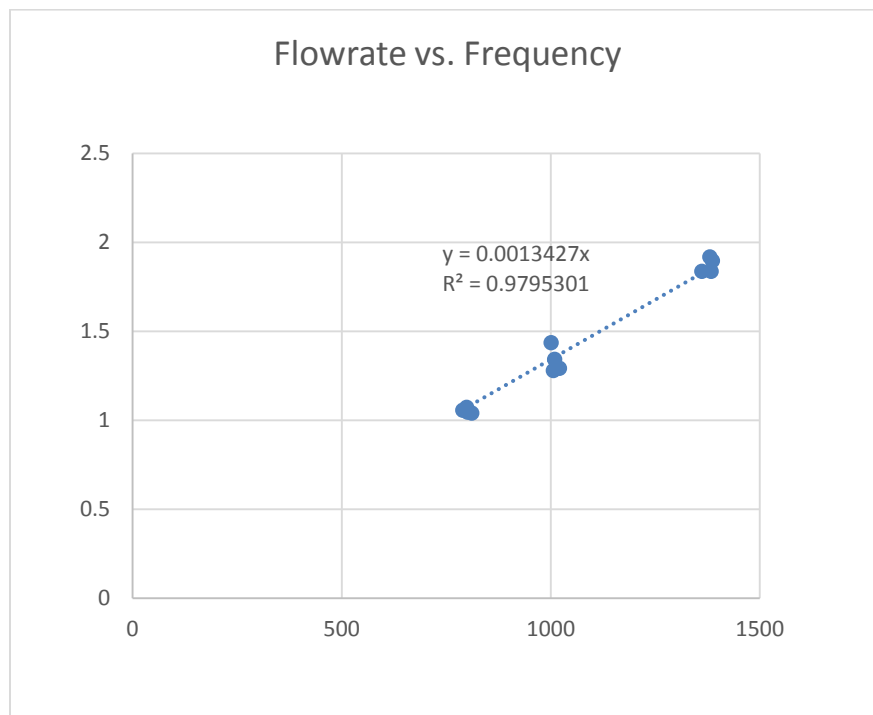
## D2.4 Calibration curve of Pressure sensor in Aortic Circulation



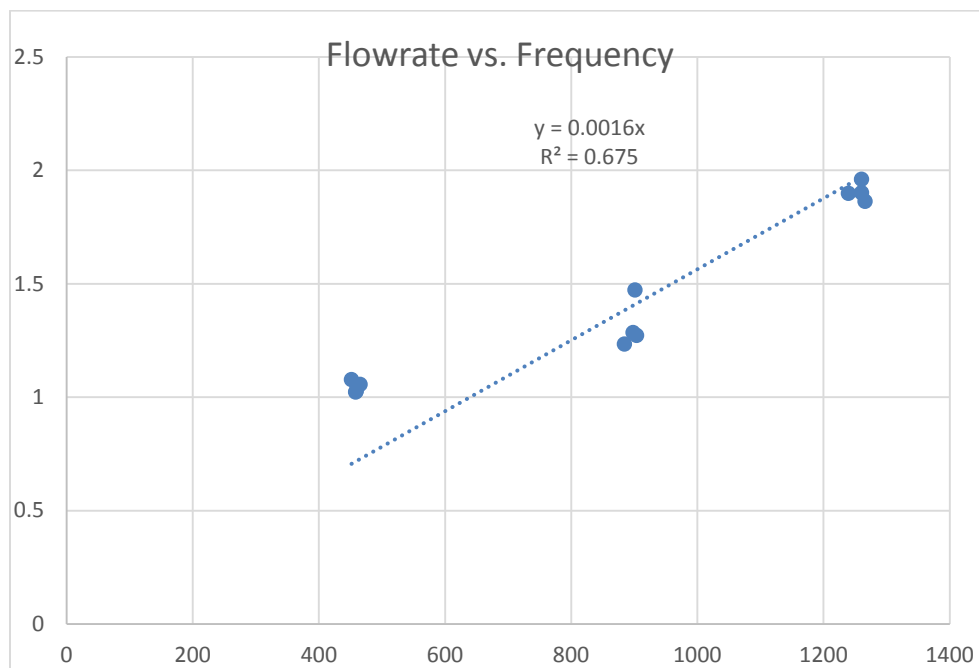
## D2.5 Calibration curve of Flow meter 1



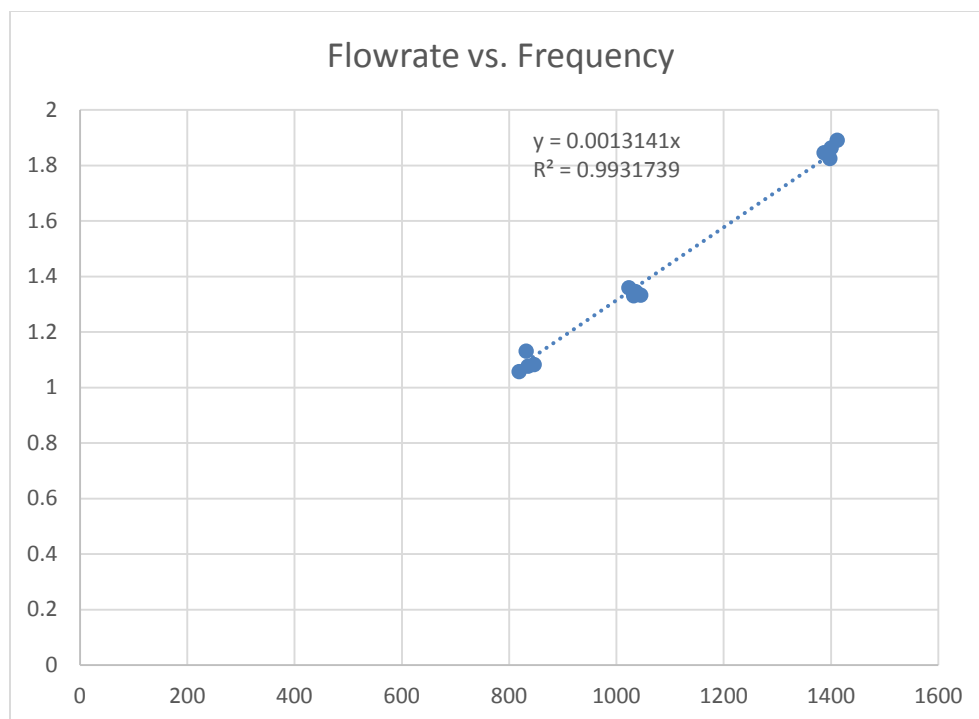
## D2.6 Calibration curve of Flow meter 2



## D2.7 Calibration curve of Flow meter 3



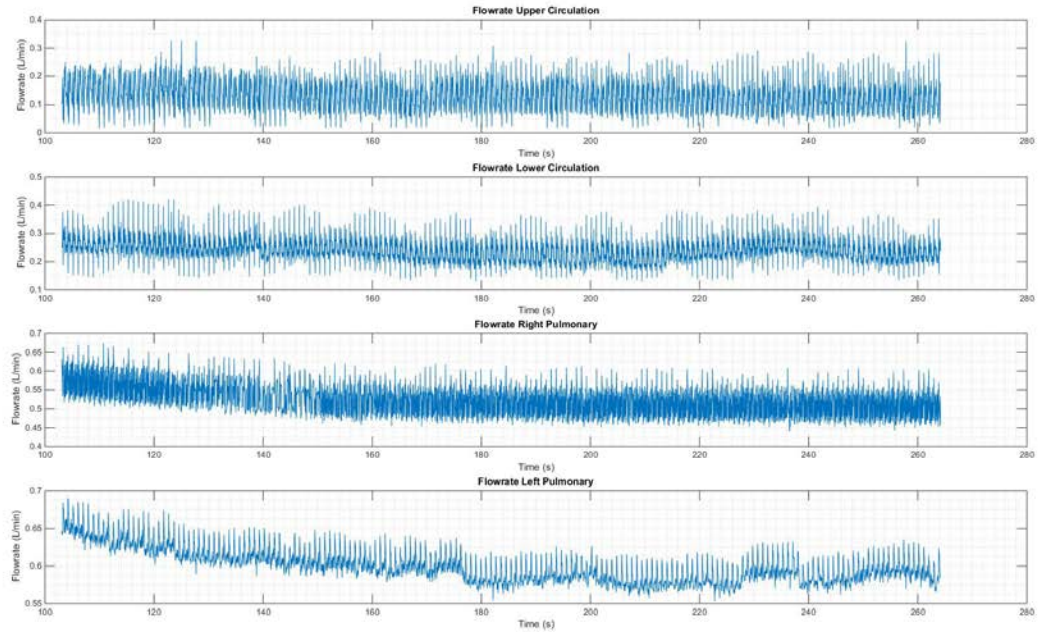
## D2.8 Calibration curve of Flow meter 4



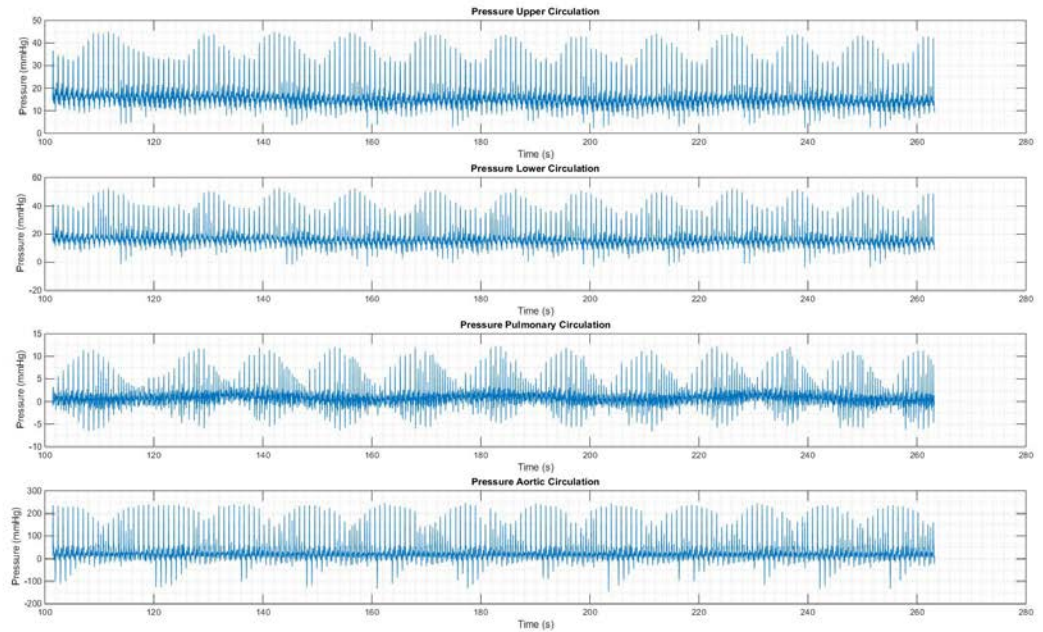
## Appendix E

### Raw Data

#### E2.1 Flow rate plots of 3mm IJS with fully open Inlet Cannula

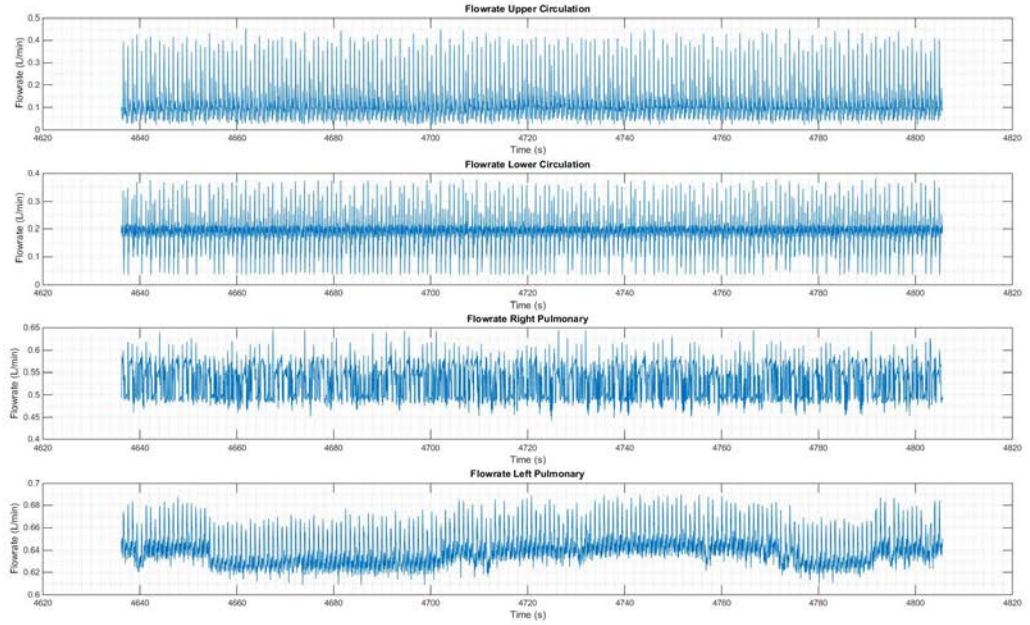


#### E2.2 Pressure plots of 3mm IJS with fully open Inlet Cannula

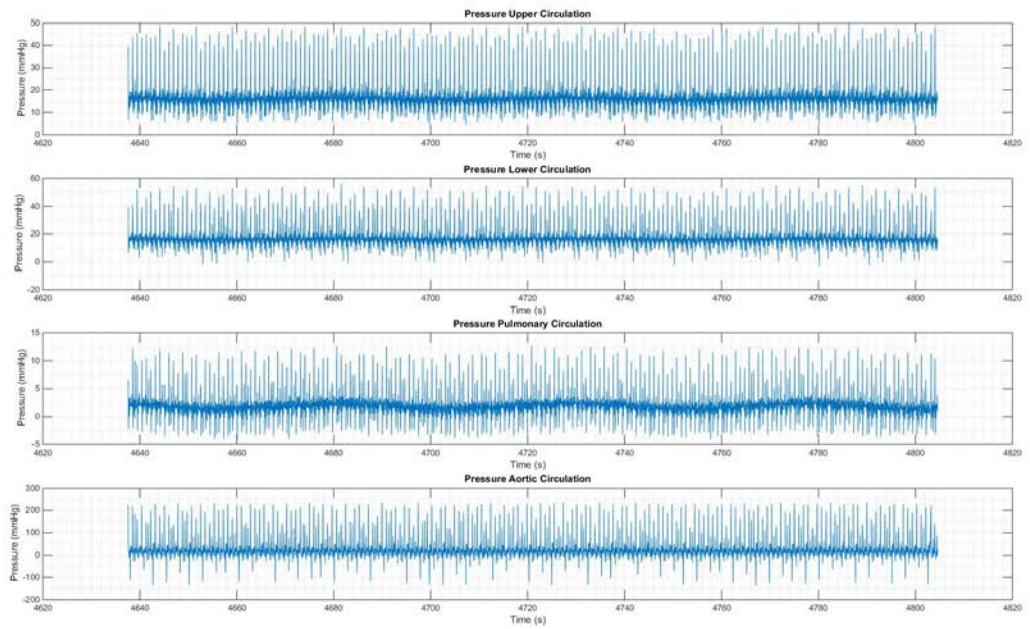




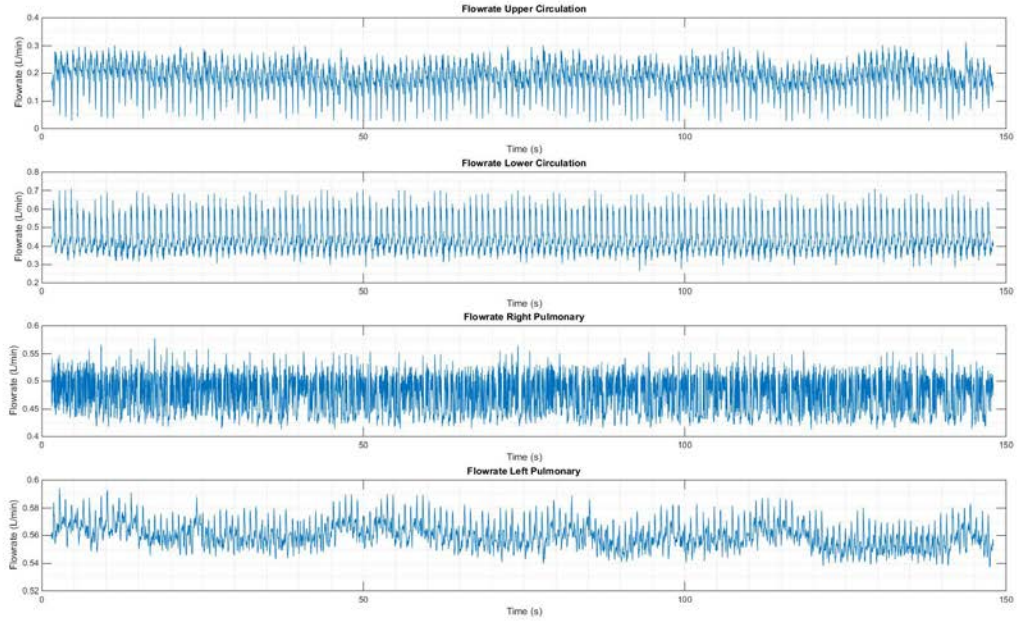
### E2.3 Flow rate plots of 4mm IJS with fully open Inlet Cannula



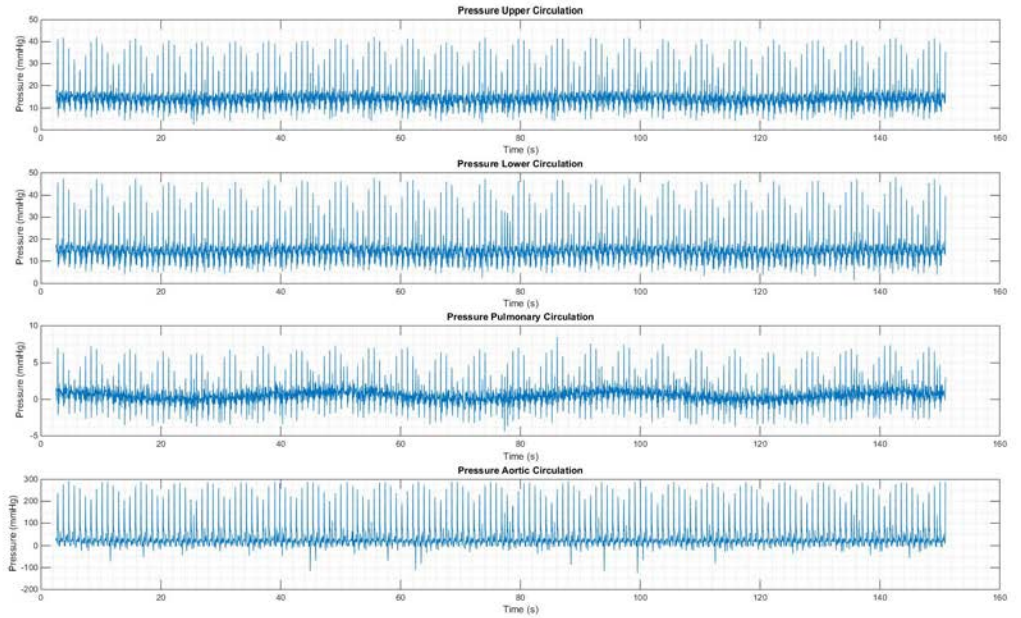
### E2.4 Pressure plots of 4mm IJS with fully open Inlet Cannula



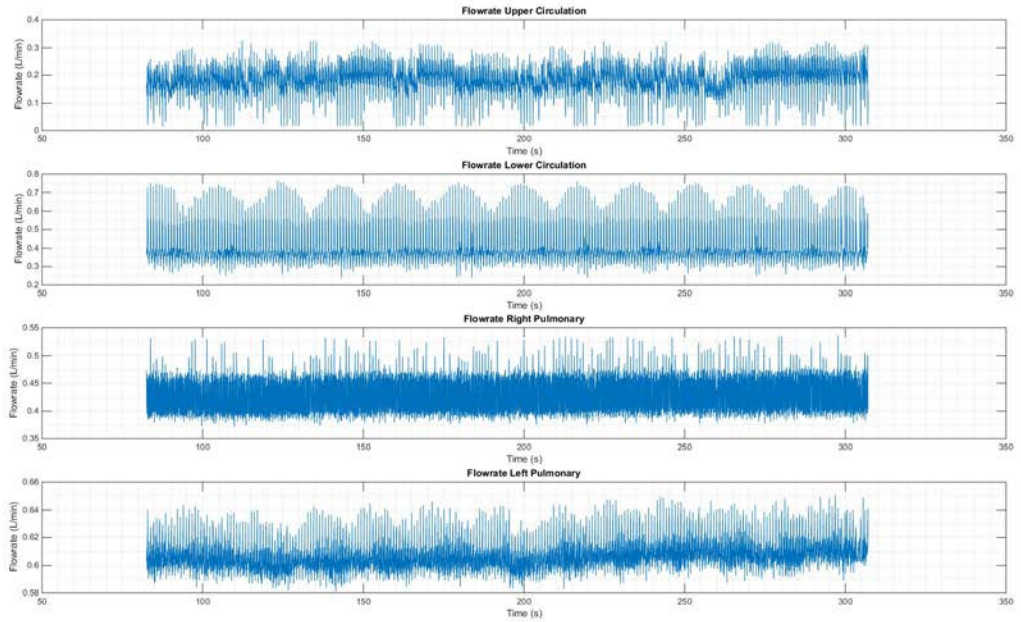
## E2.5 Flow rate plots of 3mm IJS with partially open Inlet Cannula



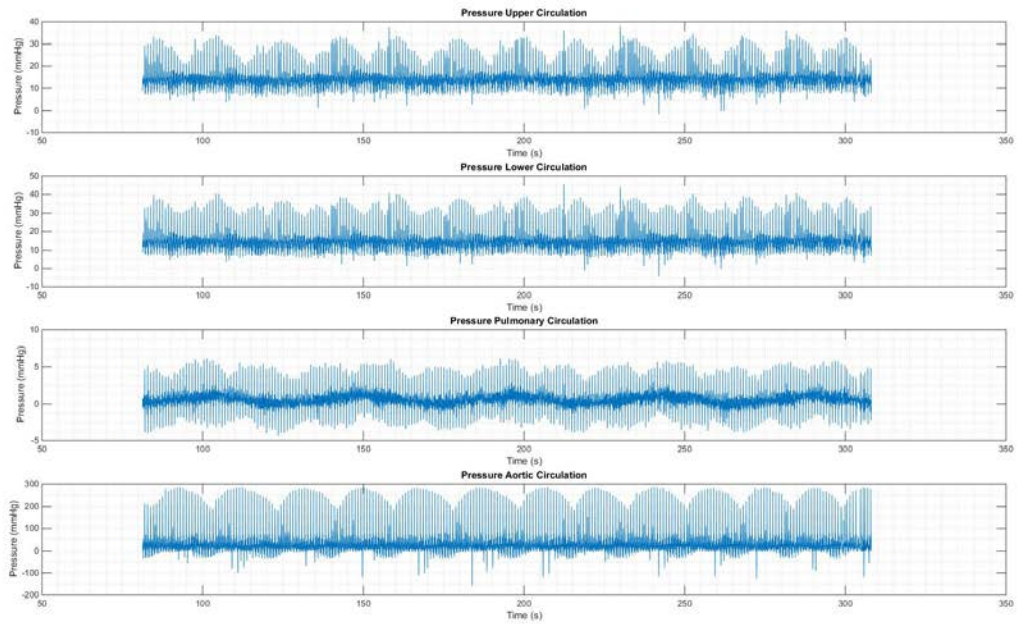
## E2.6 Pressure plots of 3mm IJS with partially open Inlet Cannula



## E2.7 Flow rate plots of 4mm IJS with partially open Inlet Cannula



## E2.8 Pressure plots of 4mm IJS with partially open Inlet Cannula



### Proposed Thesis Schedule

Milestone	Date	Initials
Submit MSA 605 Proposal for a course grade		
Rewrite Proposal and send to Committee		
Members review of Proposal (10 days)		
Chair review of Proposal (10 days)		
Rewrite Proposal		
Members approval of Proposal (10 days)		
Chair approval of Proposal (10 days)		
Completed Proposal submitted to Department		
Data Collection		
Data Analysis		
Complete Draft 1		
Committee member review of Draft 1 (10 days)		
Chair review of Draft 1 (10 days)		
Complete Draft 2		
Members review of Draft 2 (10 days)		
Chair review of Draft 2 (10 days)		
Complete final manuscript		
Members signoff of final manuscript (10 days)		
Chair signoff of final manuscript (10 days)		
Submit Word file/hard copy and paperwork to Department		
Pass/Fail grade conferred		

*Note.* Delete this page upon submission of final manuscript.